



# Oncoimmunology



ISSN: (Print) 2162-402X (Online) Journal homepage: <http://www.tandfonline.com/loi/koni20>


## Tailoring CD19xCD3-DART exposure enhances T-cells to eradication of B-cell neoplasms

Paola Circosta, Angela Rita Elia, Indira Landra, Rodolfo Machiorlatti, Maria Todaro, Sabrina Aliberti, Davide Brusa, Silvia Deaglio, Sabina Chiaretti, Riccardo Bruna, Daniela Gottardi, Massimo Massaia, Filomena Di Giacomo, Anna Rita Guarini, Robin Foà, Peter W. Kyriakides, Rohan Bareja, Olivier Elemento, Gurunadh R. Chichili, Emanuele Monteleone, Paul A. Moore, Syd Johnson, Ezio Bonvini, Alessandro Cignetti & Giorgio Inghirami

To cite this article: Paola Circosta, Angela Rita Elia, Indira Landra, Rodolfo Machiorlatti, Maria Todaro, Sabrina Aliberti, Davide Brusa, Silvia Deaglio, Sabina Chiaretti, Riccardo Bruna, Daniela Gottardi, Massimo Massaia, Filomena Di Giacomo, Anna Rita Guarini, Robin Foà, Peter W. Kyriakides, Rohan Bareja, Olivier Elemento, Gurunadh R. Chichili, Emanuele Monteleone, Paul A. Moore, Syd Johnson, Ezio Bonvini, Alessandro Cignetti & Giorgio Inghirami (2018) Tailoring CD19xCD3-DART exposure enhances T-cells to eradication of B-cell neoplasms, *Oncoimmunology*, 7:4, e1341032, DOI: [10.1080/2162402X.2017.1341032](https://doi.org/10.1080/2162402X.2017.1341032)


To link to this article: <https://doi.org/10.1080/2162402X.2017.1341032>

 View supplementary material 

 Accepted author version posted online: 05 Jul 2017.  
Published online: 08 Feb 2018.

 Submit your article to this journal 

 Article views: 96


 View related articles 

 View Crossmark data 

ORIGINAL RESEARCH



## Tailoring CD19xCD3-DART exposure enhances T-cells to eradication of B-cell neoplasms

Paola Circosta<sup>a,b</sup>, Angela Rita Elia<sup>a,b,\*</sup>, Indira Landra<sup>b,\*</sup>, Rodolfo Machiorlatti<sup>b</sup>, Maria Todaro<sup>b,c</sup>, Sabrina Aliberti<sup>b</sup>, Davide Brusa<sup>d</sup>, Silvia Deaglio<sup>d</sup>, Sabina Chiaretti<sup>e</sup>, Riccardo Bruna<sup>f</sup>, Daniela Gottardi<sup>f</sup>, Massimo Massaia<sup>f</sup>, Filomena Di Giacomo<sup>c,e</sup>, Anna Rita Guarini<sup>e</sup>, Robin Foà<sup>e</sup>, Peter W. Kyriakides<sup>c</sup>, Rohan Bareja<sup>g</sup>, Olivier Elemento<sup>g</sup>, Gurunadh R. Chichili<sup>h</sup>, Emanuele Monteleone<sup>a</sup>, Paul A. Moore<sup>i</sup>, Syd Johnson<sup>i</sup>, Ezio Bonvini<sup>i</sup>, Alessandro Cignetti<sup>a,f</sup>, and Giorgio Inghirami <sup>b,c,j</sup>

<sup>a</sup>Molecular Biotechnology Center, University of Torino, Italy, and Center for Experimental Research and Medical Studies (CeRMS), University of Torino, Torino, Italy; <sup>b</sup>Department of Molecular Biotechnology and Health Science and Center for Experimental Research and Medical Studies (CeRMS), University of Torino, Torino, Italy; <sup>c</sup>Department of Pathology and Laboratory Medicine, Weill Cornell Medicine, New York, NY, USA; <sup>d</sup>Department of Medical Sciences, University of Torino, Torino, Italy; <sup>e</sup>Flow Cytometry and Cell Sorting Facility, Human Genetics Foundation, Torino, Italy; <sup>f</sup>Division of Hematology, Department of Cellular Biotechnologies and Hematology, "Sapienza" University, Rome, Italy; <sup>g</sup>University Division of Hematology and Cell Therapy, University of Torino, Ospedale Mauriziano, Torino, Italy; <sup>h</sup>Institute for Computational Biomedicine, Department of Physiology and Biophysics, Weill Cornell Medical College, 1300 York Avenue, New York, New York, USA [2] Institute for Precision Medicine, Weill Cornell Medical College, 1300 York Avenue, New York, New York, USA; <sup>i</sup>MacroGenics Inc., 9640 Medical Center Drive, Rockville, MD, USA; <sup>j</sup>MacroGenics Inc., 9704 Medical Center Drive, Rockville, MD, USA; <sup>k</sup>Department of Pathology, NYU Cancer Center, New York University School of Medicine, New York, NY

### ABSTRACT

Many patients with B-cell malignancies can be successfully treated, although tumor eradication is rarely achieved. T-cell-directed killing of tumor cells using engineered T-cells or bispecific antibodies is a promising approach for the treatment of hematologic malignancies.

We investigated the efficacy of CD19xCD3 DART bispecific antibody in a broad panel of human primary B-cell malignancies. The CD19xCD3 DART identified 2 distinct subsets of patients, in which the neoplastic lymphocytes were eliminated with rapid or slow kinetics. Delayed responses were always overcome by a prolonged or repeated DART exposure. Both CD4 and CD8 effector cytotoxic cells were generated, and DART-mediated killing of CD4<sup>+</sup> cells into cytotoxic effectors required the presence of CD8<sup>+</sup> cells. Serial exposures to DART led to the exponential expansion of CD4<sup>+</sup> and CD8<sup>+</sup> cells and to the sequential ablation of neoplastic cells in absence of a PD-L1-mediated exhaustion. Lastly, patient-derived neoplastic B-cells (B-Acute Lymphoblast Leukemia and Diffuse Large B Cell Lymphoma) could be proficiently eradicated in a xenograft mouse model by DART-armed cytokine induced killer (CIK) cells.

Collectively, patient tailored DART exposures can result in the effective elimination of CD19 positive leukemia and B-cell lymphoma and the association of bispecific antibodies with unmatched CIK cells represents an effective modality for the treatment of CD19 positive leukemia/lymphoma.

### ARTICLE HISTORY

Received 24 April 2017  
Revised 3 June 2017  
Accepted 6 June 2017

### KEYWORDS

B-cell malignancies; bispecific antibodies; CIK cells; DART CD19xCD3; PDTX

### Key points


- CD19xCD3 DART antibodies arm CD4 and CD8 cytotoxic cells to eradicate all CD19+ lymphoproliferative disorders
- Armed CD19xCD3 DART cytokine induced killer cells can be used as universal donor cells to treat B cell neoplasms


### Introduction

The therapeutic successes achieved in the last decades in the treatment of B-cell lymphoproliferative disorders are compelling.<sup>1-6</sup>

Nevertheless, oncologists face exceeding challenges in achieving prolonged responses and cancer eradication.<sup>7-10</sup> Novel immunotherapies have proven to complement standard chemotherapy-based approaches.<sup>11-15</sup> Impressive results have been reported using engineered T-cells (CAR T-cells),<sup>16</sup> bispecific antibodies (bsAbs) and checkpoint inhibitors in the treatment of refractory/aggressive acute B-cell lymphoblastic leukemia (B-ALL) and other lymphoproliferative disorders.<sup>2,17</sup>

Among these innovative approaches, bispecific antibodies represent an exciting development, because they can be delivered off the shelf to larger cohorts of patients. Blinatumomab, a bispecific T-cell engager (BiTE) redirects T lymphocytes - irrespective of their TCR specificity- against B-cells. First

**CONTACT** Alessandro Cignetti, MD  [alessandro.cignetti@unito.it](mailto:alessandro.cignetti@unito.it)  University Division of Hematology and Cell Therapy, Ospedale Mauriziano, Via Magellano 1, 10128 Torino, Italy; Giorgio Inghirami, MD  [ggi9001@med.cornell.edu](mailto:ggi9001@med.cornell.edu)  Department of Pathology and Laboratory Medicine, Weill Cornell Medical College, 525 East 68th Street, Starr Pavilion Rm 713, New York, NY 10065 USA.

 Supplemental data for this article can be accessed on the [publisher's website](#).

\*These authors contributed equally to this work.

approved to treat Philadelphia chromosome-negative precursor B-cell ALL, blinatumomab is remarkably effective in adult B-ALL,<sup>18,19</sup> leading to clinical remission (CR) or CR with partial hematological recovery (CRh) in relapsed/refractory ALL.<sup>20</sup> BiTe-CD19xCD3 has also shown to be promising in pretreated patients with relapsed/refractory NHL,<sup>21</sup> although resistant phenotypes may emerge.<sup>22,23</sup> Since Blinatumomab treatment can be technically demanding and inconvenient for the patients, structural improvements to improve stability, unfavorable pharmacokinetics, and potential immunogenicity are desirable.<sup>24-26</sup>

Dual Affinity Re-Targeting molecules (DARTs) are flexible bsAbs-based platforms with improved stability, good heavy and light chain pairing and excellent preservation of the affinity against their target epitopes.<sup>27,28</sup> Their modular design has allowed for the rapid generation of specific DART targeting unique cancer epitopes,<sup>28,29</sup> including CD19. Although CD19xCD3 DARTs may have favorable features compared with blinatumomab<sup>29</sup> (additional stabilization through a C-terminal disulfide bridge, high stability in both formulation buffer and human serum), an in-depth understanding of the mechanisms leading to optimal DART-mediated T-cell activation and generation of potent effector cells *in vivo* are highly desirable to minimize the fraction of non-responder patients.

Several questions need to be addressed: i) the potential for an intrinsic resistant phenotype of CD19+ tumor cells; ii) the immune characteristics of cancer patients at the time of treatment and during disease progression; iii) the ideal T:B and CD4:CD8 ratio for optimal effector function *in vivo*; and iv) any potential impairment in proliferation, the occurrence of premature T-cell exhaustion, defects in cytotoxic machinery or an altered balance between killing effector memory cells and central memory cells that maintain the effector pool.

Here, we investigated the effects of CD19xCD3 DART using primary neoplastic B-cells and *in vitro* and *in vivo* models. Our findings demonstrate that CD19xCD3 DART efficiently activates both CD4<sup>+</sup> and CD8<sup>+</sup> donor T-cells that can eliminate autologous leukemia/lymphoma cells in all patients. We proved that cytokine-induced killer (CIK) cells and CD19xCD3 DART can control and/or eradicate patient-derived tumor xenografts (PDX) from chemo-refractory B-ALL and diffuse large B-cell lymphoma (DLBCL) patients. In summary, the combination of universal effector cells and CD19xCD3 DART represents a promising and powerful strategy to treat human B-cell neoplasms.

## Material and methods

### DART proteins and other materials

The CD19xCD3 DART protein was constructed as described.<sup>29</sup> The control DART molecule, 4420xCD3, in which the variable domain sequences of the anti-fluorescein mAb 4-4-20<sup>30</sup> replaces the CD19 DART protein arm, was engineered in a similar manner. DARTs were expressed transiently in CHO-S cells<sup>27</sup> and purified to homogeneity by using protein A. Dexamethasone (Sigma) and ibrutinib (Selleckchem) were used in *in vitro* assays.

### Cell lines

The human cell MEC-1 (chronic B-cell leukemia),<sup>31</sup> Daudi (Burkitt's lymphoma) and THP1 (acute monocytic leukemia) were cultured in complete RPMI 1640 (Invitrogen Life Technologies, Gaithersburg, MD) supplemented with heat-inactivated 10% fetal calf serum (FCS) and 1% penicillin/streptomycin (GIBCO, Invitrogen, Milan, Italy).

### Patients

Samples were obtained from patients hospitalized within the Division of Hematology and Cell Therapy of Ospedale Mauriziano or the Division of Hematology, San Giovanni Battista, University of Torino, Italy, after informed consent in accordance with the University and State regulations and approved by the Ethical Hospital and University committees (0081521). Diagnoses were reached according to the World Health Organization classification. Patients were selected based uniquely on CD19 expression, to widen the spectrum of B-cell malignancies. Characteristics of patients are shown in Table 1.

### Generation of CIK cells

PBMC were cultured at  $2 \times 10^6$  cells/ml in complete RPMI 1640 medium supplemented with 1000 U/ml of IFN- $\gamma$  (Pepro-Tech Inc., Rocky Hill, NJ). After 24h of culture CD3 mAb (100 ng/ml OKT3; Miltenyi Biotec, Calderara di Reno, Italy) and 300 U/ml of IL-2 (Proleukin; Chiron, Munich, Germany) were added to the cell culture. Medium was replaced (1/2) with fresh medium supplemented with IL-2 every 3rd day. Phenotypic analysis was performed at the end of 3–4 weeks of culture.

### Flow cytometric analysis

Cell surface molecules expression was determined by multicolor flow cytometry, using a panel of monoclonal antibodies (see supplemental data).

### B-cell depletion assay

Mononuclear cells were isolated from bone marrow (BM) or peripheral blood (PBMC) by Ficoll-paque gradient (Pharmacia, Uppsala, Sweden) and re-suspended in complete RPMI 1640 at  $1 \times 10^6$ /ml. B-ALL were cultured in complete Iscove's Modified Dulbecco's Media (Invitrogen Life Technologies).

4420xCD3 or CD19xCD3 DART (0,1 ng/ml to 10 ng/ml) were maintained for 6 d. Viable cells was determined by trypan blue staining. The fold changes were calculated as described in supplemental data. In repetitive cell cultures of primary B-CLL, CD19xCD3 DART-expanded T-cells were re-challenged with autologous purified CD19<sup>+</sup> B- cells ( $1 \times 10^6$ /ml).

### Proliferation

The proliferation of autologous T-cells was evaluated by flow cytometer. Labeled PBMC with CFSE (see supplemental data) were plated at  $1 \times 10^6$ /ml in RPMI 1640 and cultured with or without CD19xCD3 or 4420xCD3 DART for 6 consecutive

**Table 1.** Characteristics of patients.

UPN	SOURCE	WHO 2008 CLASSIFICATION	DISEASE STATUS	%CD4 at day 0	%CD8 at day 0	%CD19 at day 0
PT# 1	SPL	B Splenic Lymphoma (not classified)	DGN	2.3	2	92
PT# 2	LN	B-CLL	DGN	N/A	N/A	N/A
PT# 3	LN	B-CLL	DGN	21	4.5	74
PT# 4	LN	FL	R/R (I REL)	N/A	N/A	N/A
PT# 5	LN	MCL	R/R (I REL)	N/A	N/A	N/A
PT# 6	LN	B-CLL	UNTREATED	9	3	87
PT# 7	LN	FL	DGN	50	21	26
PT# 8	PB	FL	DGN	21.21	4.84	60.55
PT# 9	PB	B-CLL	UNTREATED	2.99	1.53	91.95
PT#10	PB	SMZL	UNTREATED	3.66	1.95	55.8
PT#11	PB	B-CLL	R/R (REF)	1.45	0.37	96.39
PT#12	BM	B-CLL	R/R (REL)	3.5	6	90
PT#13	PB	B-CLL	R/R (REF)	2.67	1.98	87.94
PT#14	PB	B-CLL	R/R (II REL)	0.8	0.5	98
PT#15	LN	FL	DGN	3.52	0.89	86.26
PT#16	PB	B-CLL	R/R (I REL)	11.85	9.6	71.33
PT#17	PB	B-CLL	R/R (III REL)	2.88	2.01	89.14
PT#18	PB	MCL	DGN	3.26	7.33	85.38
PT#19	PB	FL	DGN	4.45	1.06	94.76
PT#20	BM	B-ALL	DGN	3.65	3.16	84.57
PT#21	PB	SMZL	R/R (REL)	56.55	16.88	12.25
PT#22	PB	B-CLL	R/R (REL)	0.43	0.22	98.72
PT#23	PB	B-CLL	UNTREATED	2.28	2.02	88.3
PT#24	PB	SMZL	DGN			
PT#25	PB	B-CLL	R/R (II REL)	4.52	2.99	91.1
PT#26	PB	B-CLL	R/R (REF)	11.61	9.8	69.46
PT#27	PB	B-ALL	DGN	1.33	0.66	72.87
PT#28	BM	HCL	DGN	11.03	2.64	75.69
PT#29	LN	DLBCL	DGN	51.75	21.1	16.8
PT#30	BM	MCL	DGN	16.43	5.38	44.46
PT#31	PB	MZL	R/R (REF)	2.44	8.06	63.44
PT#32	PB	B-ALL	DGN	1.52	0.51	94.77
PT#33	PB	B-CLL	DGN	6	6.13	79.47
PT#34	PB	B-ALL	DGN	1.04	1.11	90.33
PT#35	PB	B-ALL	DGN	2.74	2.08	83.98
PT#36	PB	B-CLL	R/R (I REL)	2.04	3.59	87.89
PT#37	PB	B-ALL	R/R (REF)	2.94	5.82	84.63
PT#38	BM	B-CLL	R/R (II REL)	1.4	0.7	98
PT#39	PB	FL	DGN	28.65	4.38	41.99
PT#40	PB	B-CLL/Richter transformation	R/R (REF)	0.61	0.26	98.46
PT#41	PB	B-CLL	R/R (I REL)	11.63	11.15	74.09
PT#42	PB	B-CLL	DGN	6.06	2.23	88.53
PT#43	PB	blastoid MCL	DGN	2.28	0.91	81.01
PT#44	BM	B-ALL	DGN	0.27	0.39	98.08
PT#45	PB	MZL	R/R (II REL)	11.1	4.58	66.24
PT#46	BM	B-CLL	DGN	5.61	3.29	69.28
PT#47	PB	B-CLL	DGN	5.32	3.17	87.19
PT#48	PB	B-CLL	DGN	19.72	2.1	66.9
PT#49	BM	B-CLL	DGN	4.27	2.07	79.35
PT#50	PB	MCL	DGN	1.28	1.16	96.74

days. At the end of cultures, CD19 B-cells were monitored and proliferation of redirected T-cells was quantified on viable cells as % of CD4<sup>+</sup>CSFE<sup>-</sup> or CD8<sup>+</sup>CSFE<sup>-</sup> cells.

### Cytokine production

Measurement of IFN- $\gamma$ , TNF $\alpha$ , IL-10, IL-6, IL-4, IL2 in tissue culture supernatants was performed using available ELISA set (CBA assay) according to the manufacturer's recommendations. Supernatants were collected from cultured cells at day 6. The results were interpolated from a standard curve using recombinant cytokines and expressed in pg/ml.

### In vivo efficacy studies

NOD.Cg-Prkdc<sup>scid</sup> Il2rg<sup>tm1Wjl</sup>/SzJ (NSG) mice were bred within the Molecular Biotechnology Center (MBC) Animal Resource,

under strict specific and opportunistic pathogen free (SOPF) conditions. Patient Derived Tumor Xenograft (PDTX) were established as described<sup>32</sup> and mice were treated with CIK with and without DART antibodies (see supplemental data). Mouse studies were executed in accordance to the animal experiment design within the project entitle "Analysis of the molecular aberration of solid tumors and lymphoproliferative disorders" approved by the Bioethical Committee of the University of Torino (Torino, September 11, 2010).

### Magnetic resonance imaging

Whole-body Magnetic Resonance images (MRI) of anesthetized (Zoletil 100 at 20 mg/kg, Rompun at 5 mg/kg.) NSG grafted mice with B-ALL were acquired on the M2 Aspect 1T MRI scanner (Aspect Imaging, Shoham, Israel) equipped with a 30 mm solenoid RX/TX coil. T<sub>2</sub>-weighted anatomic images

were acquired with a Fast Spin Echo sequence (TR/TE/NEX 2800 ms/44 ms/2) covering 21 slices (thickness 1 mm, gap 0.1 mm, Field of View 100 mm and Matrix Size 256, for an in-plane resolution of 391  $\mu\text{m}$ ). Images were manually segmented using 3D Doctor Able software to calculate the volume of target organs for 3D rendering.

### **RNA-Seq library preparation and RNA-Seq analysis and Gene expression profile analysis**

RNA-seq was performed as described previously<sup>32</sup> (see supplemental data). Hierarchical clustering and dendrogram were generated by means of the GenePattern2.0 suite. Gene set enrichment analyses were performed by means of GSEA software.<sup>33</sup>

### **Statistical analysis**

Statistical analysis was performed by Prism software, version 5.0 (GraphPad Software, San Diego, CA). Data are reported as means  $\pm$  SD or means only, as described in figure legend (see supplemental data).

## **Results**

### ***In vitro* response to CD19xCD3 DART stratifies B-cell lymphoproliferative disorders in 2 distinct subsets**

To assess the activity of CD19xCD3 DART against primary lymphoproliferative cells, we selected 50 naïve or treated patients (25 B-chronic lymphocytic leukemia, 7 B-ALL, 6 follicular lymphoma, 5 marginal zone lymphoma, 5 mantle cell lymphoma, 1 hairy cell leukemia, 1 patient with splenic lymphoma NOS). The percentage of B-cells ranged from 12.25% to 98.72% (median 85.01%) with a broad B:T ratio (0.16 to 151.87; median 12.26). Relevant clinical and phenotypic characteristics are reported in Table 1.

When unfractionated samples were cultured with increasing concentrations of CD19xCD3 DART (from 0.1 ng/ml to 10 ng/ml) or control DART (4420xCD3) or in supplemented medium, a decrease in CD19 cells was observed only in the CD19xCD3 DART treated samples (Fig. 1A). Percentage of CD19<sup>+</sup> B-cells (killing percentage) correlated with the B:T ratio at day 0 ( $r_s = \sim -0.73$ ,  $p = 9.8 \times 10^{-9}$ ). As the extent of B-cell depletion observed at 10 ng/ml DART was variable (mean of 17.88% CD19<sup>+</sup> B-cells), samples were stratified according to the CD19 mean value (at day 6, < or > 17.88%). Patients with CD19 B-cell ratios greater than 17.88% were defined as “slow responders” and those with less than 17.88% as “fast responders.” Fast responders showed a significant reduction in B-cells (Fig. 1B top panel), compared with slow responders or controls (Fig. 1B bottom panel). Similar results were obtained grouping patients according to the CD19<sup>+</sup> percentage at day 6 and focusing on upper (25<sup>th</sup>) and lower distribution (75<sup>th</sup>). A representative dot plot of a fast responder (PT# 19 top panel) and slow responder patient (PT# 15 bottom panel) is shown (Fig. 1C).

CD19xCD3 DART elicited a robust expansion of both autologous CD4<sup>+</sup> and CD8<sup>+</sup> autologous lymphocytes (Fig. 1D–1G,

S1-A), with an increase in the absolute numbers of T-cells (Fig. 1E) and a net reduction/complete depletion of B-cells. We observed a less noticeable CD4<sup>+</sup> and CD8<sup>+</sup> expansion among slow responders (Fig. 1F). Moreover, the absolute numbers of CD4<sup>+</sup> cells (Fig. 1G left panel), but not that of CD8<sup>+</sup>, increased in the slow responders compared with controls (Fig. 1G right panel), suggesting that CD8<sup>+</sup> effector T-cells are required for an effective ablation of the target cells. Since the percentage of CD4<sup>+</sup> and CD8<sup>+</sup> T-cells at day 0 was substantially higher within the fast responders’ group (CD4:  $11.04 \pm 14.96$  vs  $4.36 \pm 5.67$  and CD8:  $5.33 \pm 5.4$  vs  $1.62 \pm 1.63$  with  $p = 0.03$  for CD4<sup>+</sup> and  $p = 0.0009$  for CD8<sup>+</sup>, respectively), we correlated the percentage of CD19<sup>+</sup> cells at day 6 with CD3<sup>+</sup> T-cells (CD4<sup>+</sup> and CD8<sup>+</sup>) at day 0 ( $r_s = -0.3237146$ ,  $p \sim 0.02$ ), suggesting that CD19xCD3 treatment is affected by the initial number of CD3<sup>+</sup> T-cells. This was corroborated by designing a random effect mixed model allowing for subject dependent effects (LRT:  $p = 0.0008605$  \*\*\*).

Next we tested whether CD19xCD3 DART treated T-cells maintained their specificity, avoiding off target effect. We mixed CD19xCD3 DART or control-challenged T-cells with CD19<sup>+</sup> MEC-1 cells at different effector: target (E:T) ratios. Negligible lysis of MEC-1 cells was observed at lower ratio (E:T 0,62:1:  $17.95 \pm 11.38\%$ ), but lysis was seen at higher E:T ratios ( $91.3 \pm 4.8\%$  at 20:1  $P = < 0.0001$ , Fig. S1-B), an effect that could be blocked by a neutralizing anti-CD19 Abs (Fig. S1-C) and in part linked to membrane bound CD19xCD3 DART molecule (Fig. 1S–D) Conversely, minimal cell lysis was seen at the highest E:T ratios ( $21.93 \pm 13.20$ ) using CD19 negative target-cells (THP1).

### ***Total B-cell eradication can be achieved in both fast responder and slow responder patients***

Since treatment of slow responders with CD19xCD3 DART could lead to a partial eradication, we assessed their T-cell expansion capacity in randomly selected patients, demonstrating that CFSE labeled CD4<sup>+</sup> and CD8<sup>+</sup> cells effectively proliferate in the presence of CD19xCD3 DART (Fig. 2A left and right panel) and that prolonged exposures (12 days) to CD19xCD3 were associated with their robust expansion (Fig. 2B middle and right panel) and complete eradication of neoplastic B-cells (5 B-CLL, 1 B-ALL, Fig. 2B left panel). In very poor responders, a further challenge (on day 14) with the CD19xCD3 DART was necessary (Fig. 2C, left panel), leading to global T-cells expansion with a rapid CD4<sup>+</sup> growth (Fig. 2C, middle panel) and a more progressive CD8<sup>+</sup> cells expansion (Fig. 2C, right panel).

Next, we tested whether the exposure to dexamethasone could modulate the efficacy of CD19xCD3 DART. As corticosteroids are used to prevent cytokine release syndrome (CRS), we pre-treated PBMC with dexamethasone and then we added the DARTs. The pretreatment blocked the expansion of autologous T-cells and the eradication of neoplastic B-cells (DART  $3 \pm 4.9$  versus DART + dexametasone  $80.84 \pm 8.85$ , Fig. 2D, left panel). Conversely, when we first treated the PBMC with DARTs and then added the dexamethasone, we did not observe any loss of the activation of autologous T-cells and the

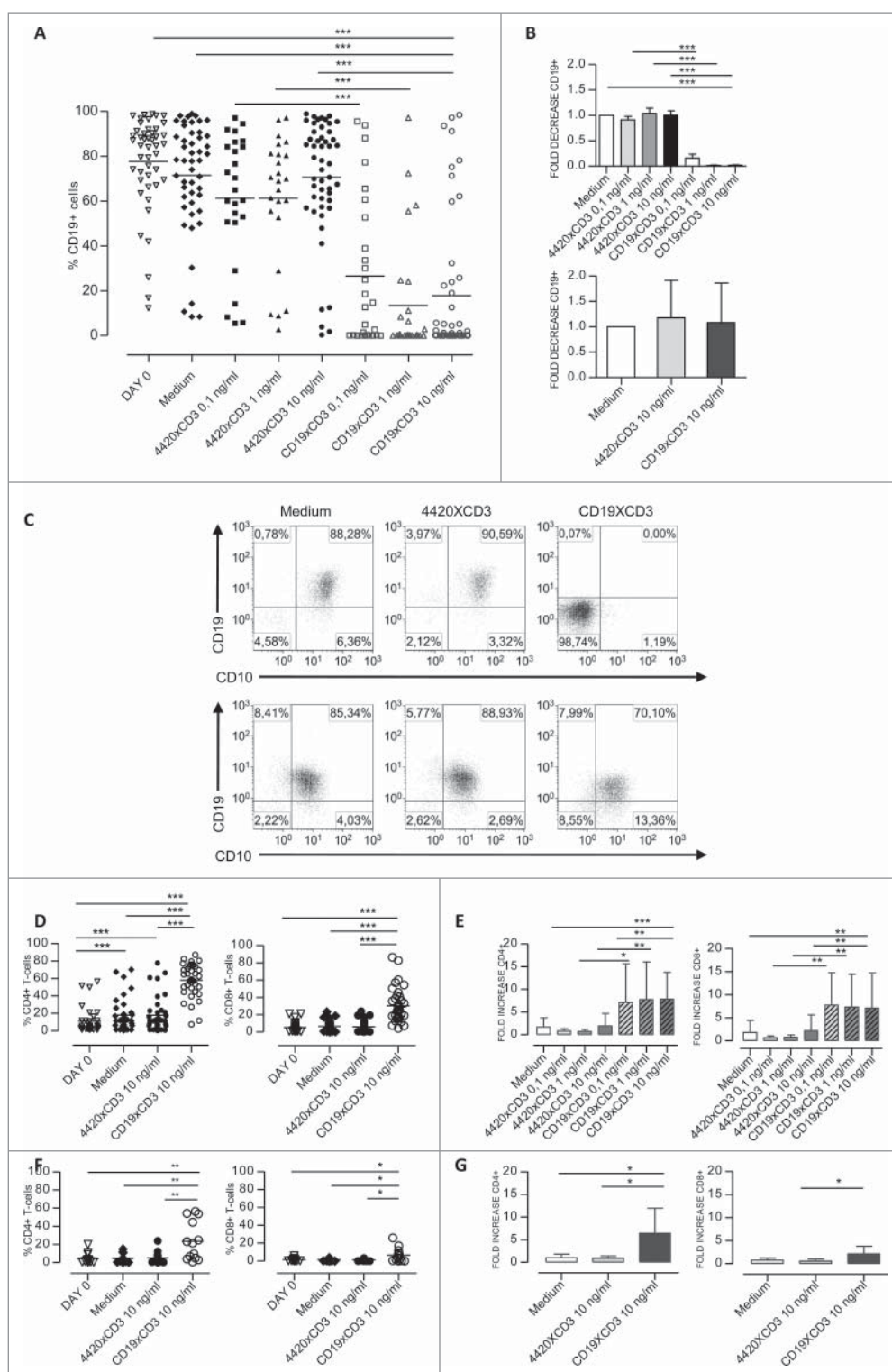


**Figure 1.** CD19xCD3 molecule mediates autologous CD19<sup>+</sup> B-cells depletion and expansion of T-cells *in vitro*. (A) PBMC from PB, BM, spleen or lymph node (n = 50) were incubated for 6 d alone, with 4420xCD3 or with CD19xCD3 DART (0.1ng/ml, 1ng/ml and 10ng/ml). The percentage of CD19<sup>+</sup> was evaluated by flow cytometry on viable cells. The horizontal bars indicate the median value. \*\*\*P < 0.001. (B) The fold change of B-cells was determined at day 6 as the ratio between the absolute number of CD19<sup>+</sup> cells in CD19xCD3 DART cultures and CD19<sup>+</sup> cells cultured with medium alone. The graphs represent the fold decrease of CD19<sup>+</sup> in fast responders (top panel, n = 8) and in slow responders (bottom panel, n = 8). The fold changes of fast responders and slow responders at 10 ng/ml were 0.018 ± 0.04 and 1.0 ± 0.83 \*\*\* P < 0.001. (C) Flow cytometry of a representative fast (top panel) and slow responder patient (bottom panel). (D) The percentage of CD4<sup>+</sup> (left panel) CD8<sup>+</sup> (right panel) of fast responder patients (n = 37). The horizontal bars indicate the median value. (\*\*\*)P < 0.001; CD4<sup>+</sup> from 11.04 ± 14.96 at day 0 to 58.07 ± 19.11, CD8<sup>+</sup> from 5.33 ± 5.4 to 30.24 ± 19.31 at day 6). (E) The fold change of T-cells was determined as the ratio between absolute number of CD4<sup>+</sup> or CD8<sup>+</sup> cells in CD19xCD3 DART cultures at day 6 and at day 0. The fold changes of fast responders CD4<sup>+</sup> were 7.84 ± 5.9 (left panel) and CD8<sup>+</sup> 7.09 ± 7.6 (right panel, n = 23). \*\*P < 0.01, \*\*\*P < 0.001. (F) The percentage of CD4<sup>+</sup> (left panel) CD8<sup>+</sup> (right panel) of slow responder patients (n = 13). Horizontal bars represent the median values (CD4<sup>+</sup> changed from 4.36 ± 5.67 at day 0 to 22.63 ± 21.47 and CD8<sup>+</sup> from 1.62 ± 1.63 to 6.62 ± 7.69). \*P < 0.05 and \*\*P < 0.01. (G) The fold change of T-cells was determined as the ratio of absolute number of CD4<sup>+</sup> or CD8<sup>+</sup> cells in CD19xCD3 DART cultures between day 6 and day 0. The fold changes of slow responder CD4<sup>+</sup> were 6.39 ± 5.56 (left panel) and CD8<sup>+</sup> 2.13 ± 1.66 (right panel, n = 8). \*P < 0.05 Student's t test.

eradication of neoplastic B-cells occurred (Fig. 2D middle panel). Similarly, T-cells of ibrutinib-treated CLL patients were functional once challenged with the bsAbs in the absence of the TKi (Fig. 2E). Interestingly, CD8<sup>+</sup> cells of ibrutinib-treated patients were more efficient effectors than those of naïve patients (treated 41.41 ± 11.13 vs. untreated 24.10 ± 19.95).

**CD19xCD3 DART promotes T-cell activation and differentiation**

To define the mechanisms leading to DART-mediated T-cell activation, we first assessed the cytokine levels of supernatants triggered by CD19xCD3 DART or control DART-cells. High

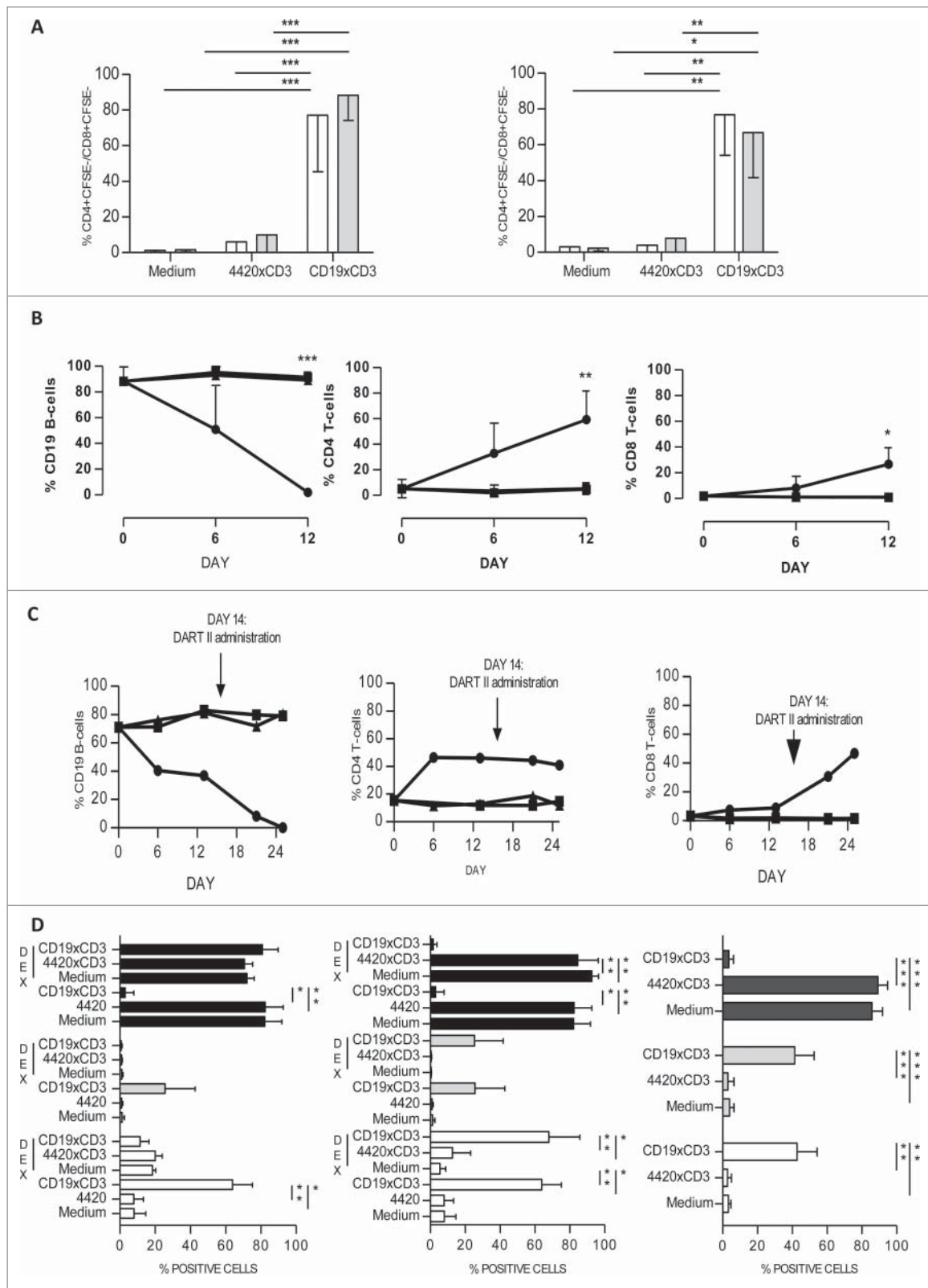


Figure 2. (For figure legend, see page 7.)

levels of IFN- $\gamma$ , TNF- $\alpha$ , IL10, and IL6 were produced after DART activation (Fig. S2-A)<sup>34,35</sup> by T-cells which rapidly upregulated CD25 surface membrane receptors (Fig. S2-B). Acknowledging that CD4<sup>+</sup>CD25<sup>+</sup> T-cells can be negative regulators, we quantified CD4<sup>+</sup>CD25<sup>+</sup>FoxP3<sup>+</sup> among DART activated T-cells, demonstrating only seldom and minor expansions (Fig. 3A). Conversely, CD4<sup>+</sup> and CD8<sup>+</sup> co-expressed PD-1 (Fig. 3B), a marker linked to either activation or T-cell exhaustion.<sup>36</sup> Then, when PD-1<sup>+</sup> and PD-1<sup>-</sup> cells were isolated and co-cultured with CD19<sup>+</sup> MEC-1 target-cells, they displayed similar efficacies (Fig. 3C), suggesting that the PD-1 expression was not linked to a dysfunctional phenotype.

Immunophenotypically DART activated CD4<sup>+</sup> and CD8<sup>+</sup> displayed a central and effector memory phenotype (Fig. 3D left and right panel,  $P < 0.05$  and Fig. 3E left and right panel), while terminally differentiated effector memory subsets (TEMRA CD45RA<sup>+</sup>CD62L<sup>-</sup>) represented a small fraction. Similar findings were seen in slow responders.

Interestingly, CD8<sup>+</sup> expressed higher levels of granzyme B than CD4<sup>+</sup> T-cells (Fig. 3F) and lesser CD4<sup>+</sup> (mean:  $4.81 \pm 4.29$ ) and CD8<sup>+</sup> (mean:  $35.63 \pm 11.76$ ) granzyme<sup>+</sup> cells were observed in slow responders (CD4<sup>+</sup> mean:  $12.78 \pm 5.48$ ; CD8<sup>+</sup> mean:  $64.04 \pm 18.6$ ). We also noted that the DART-mediated responses could change over time, as documented in a patient that, during the course of the disease, displayed both phenotypes (Fig. 3G, upper and lower panel).

To gain further insight into the mechanisms related to the functional changes in T-cells after DART-mediated activation, we performed transcriptomics analyses of purified cells prior and after CD19xCD3 DART exposure. Unsupervised analysis showed that CD19xCD3 DART-activated CD4<sup>+</sup> and CD8<sup>+</sup> cells clustered together and displayed high levels of genes expressed by memory, Th1 and cytotoxic T-cells (Fig. 3H to L). CD19xCD3 DART CD4 cells were positive for ThPOK, GATA3, Myb and RUNX1 transcription factors, known to control the CD4 phenotype, and STAT1, STAT3, 4 and 5. STAT1 regulates the expression of T-Bet which in conjunction with STAT4 leads to the upregulation of RUNX3. These findings were also in agreement with the increased expression of IFN- $\gamma$  by CD19xCD3 DART activated CD4 cells (Fig. 3L).

### Both CD4<sup>+</sup> and CD8<sup>+</sup> cells differentiate into effector cytotoxic elements and maintain their cytotoxic capacity upon consecutive challenges

Following CD19xCD3 DART, purified CD8<sup>+</sup> cells were rechallenged with CD19<sup>+</sup> cells (Fig. 4A) and demonstrated a robust cytotoxic response with or without further addition of the CD19xCD3 DART. Conversely, purified CD4<sup>+</sup> T-cells displayed a minor cytotoxic capacity in the absence of DART (E:T ratio 20:1:  $41.44 \pm 23.34$ ) but the addition of CD19xCD3 DART improved target elimination (Fig. 4A).

To test whether CD4<sup>+</sup> and CD8<sup>+</sup> cells were concomitantly required for the generation of effector cytotoxic cells, purified CD4<sup>+</sup> or CD8<sup>+</sup> cells at day 0 were mixed with autologous B-cells in the presence of CD19xCD3 DART. Under these conditions, CD8<sup>+</sup> were effective in killing the target T-cells, while CD4<sup>+</sup> cytotoxic activity was absent (Fig. 4B). Overall, these data demonstrate that the generation of CD4<sup>+</sup> cytotoxic cells requires the concomitant presence of the CD8<sup>+</sup> elements.

Next, to test whether CD19xCD3 DART-mediated T-cells could be maintained over time, we selected a responder patient (PT#6) whose DART-activated T-cells were repeatedly challenged with freshly isolated autologous purified CD19<sup>+</sup> (1:5 ratio E:T, Fig. 5A). This protocol was repeated up to 7 consecutive times, demonstrating that DART-activated cells could maintain their cytotoxic capacity and be able to eradicate neoplastic B-cells for up to 7 consecutive re-challenges (Fig. 5B, lower panel). Conversely, untreated or 4420xCD3 DART-challenged T-cells were ineffective (Fig. 5B). CD19xCD3 DART re-stimulation was associated with a robust T-cell expansion (Fig. 5C), high levels of IFN $\gamma$  and TNF $\alpha$  (Fig. S3-A) and by accumulation of granzyme B-positive CD4<sup>+</sup> and CD8<sup>+</sup> cells (Fig. 5D).

### CD19xCD3 DART exhibits antitumor effects in xenograft mouse models

To extend our *ex vivo* data, we studied 2 humanized mouse models bearing Patient Derived Tumor Xenograft (PDTX). Since human PMBC lead to severe graft vs. host disease (GVHD) in NOD.Cg-Prkdcscid Il2rgtm1Wjl/SzJ (NSG) mice,<sup>37</sup> we applied an alternative strategy taking advantage of human cytokine-induced killer (CIK) effector cells. CIK

**Figure 2.** (see previous page) CD19xCD3 DART induces proliferation of CD4<sup>+</sup> and CD8<sup>+</sup> cells and leads to total eradication of neoplastic B-cells in fast responder and slow responder patients. (A) CFSE<sup>+</sup> PMBC of fast responder (n = 8) or slow responders (n = 4) patients were cultured in media, with 4420xCD3 or CD19xCD3 DART at 10 ng/ml, for 7 d. The graphs show the percentage of dividing CD4<sup>+</sup> (white column) or CD8<sup>+</sup> (gray column) of responder (left panel) or slow responder patients (right panel, CD4<sup>+</sup>:  $77.08 \pm 31.82$  vs  $76.73 \pm 22.64$  and CD8<sup>+</sup>:  $88.23 \pm 14.24$  vs  $66.74 \pm 25.18$ ). Statistical significance: \* $P < 0.05$ , \*\* $P < 0.01$ , \*\*\* $P < 0.001$ . (B) PMBC from slow responder patients (n = 6) were cultured alone (■), with 4420xCD3 (▲) or CD19xCD3 at 10ng/ml (●) for the indicated number of days. The percentage of CD19<sup>+</sup> B-cells (left panel), CD4<sup>+</sup> (middle panel) or CD8<sup>+</sup> T-cells (right panel) is presented. Asterisks represent statistical significance of CD19<sup>+</sup>, CD4<sup>+</sup> or CD8<sup>+</sup> T-cells cultured with CD19xCD3 DART vs untreated (B-cells: from  $50.84 \pm 34.36$  at day 6 to  $1.88 \pm 2.18$  at day 12, CD4<sup>+</sup> from  $32.91 \pm 23.64$  at day 6 to  $59.30 \pm 22.38$  at day 12; CD8<sup>+</sup>: from  $8.14 \pm 9.21$  at day 6 to  $26.73 \pm 12.82$  at day 12; \* $P < 0.05$ , \*\* $P < 0.01$ , \*\*\* $P < 0.001$ ) (C) PMBC of a single slow responder patient were cultured either alone (■), with 4420xCD3 (▲) or with CD19xCD3 (●) at 10 ng/ml up to day 13 (CD19<sup>+</sup> cells from 71.10% at day 0 to 40.37% day 6). On day 14 cultured cells were harvested and re-challenged with DART at 10 ng/ml. At day 6, 13, 21, 25 the percentage of viable CD19<sup>+</sup> (left panel), CD4<sup>+</sup> (middle panel) or CD8<sup>+</sup> (right panel) cells was determined. The percentage of CD4<sup>+</sup> increased from 15.44% at day 0 to 45.86% at day 13, 44.22% at day 21 and 40.84% at day 25. The percentage of CD8<sup>+</sup> increased from 3.21% at day 0 to 8.77% at day 13, 30.81% at day 21 and 46.71% at day 25. (D) Left panel: PMBC from B-CLL patients were cultured with dexamethasone at  $10^{-5}$ M for 3 d and then 4420xCD3 or CD19xCD3 DART at 10 ng/ml were added for 4 d. In control cultures, PMBC were incubated for 7 d either alone, with 4420xCD3 at 10ng/ml or CD19xCD3 DART at 10 ng/ml. The percentage of CD4<sup>+</sup> (white column), CD8<sup>+</sup> (gray column) and CD19<sup>+</sup> (black column) are depicted. The treatment with the corticosteroid blocked the expansion of CD4<sup>+</sup> (DART-treated  $63.9 \pm 11.3$  vs. DART+ dexametasone  $11.47 \pm 5.08$ ) and CD8<sup>+</sup> (DART-treated  $25.67 \pm 16.9$  vs. DART+ dexametasone  $0.7 \pm 0.5$ ) cells and impaired the eradication of neoplastic B-cells (DART  $3 \pm 4.9$  vs. DART+ dexametasone  $80.84 \pm 8.85$ ). Right panel: PMBC were cultured with 4420xCD3 or CD19xCD3 DART at 10 ng/ml for 3 d and then dexamethasone at  $10^{-5}$ M was added for 4 d. Dexamethasone treatment after DART led to activation of autologous T-cells (CD4<sup>+</sup>:  $67.9 \pm 17.8$  and CD8<sup>+</sup>:  $25.34 \pm 16.45$ ) and the eradication of the neoplastic B-cells ( $1.59 \pm 2.14$ , \* $P < 0.05$ , \*\* $P < 0.01$ , \*\*\* $P < 0.001$ ). (E) PMBC from B-CLL patients under treatment with ibrutinib at therapeutic dose (n = 5) were incubated for 6 d either alone, with 4420xCD3 or with CD19xCD3 DART at 10ng/ml. Percentage of CD4<sup>+</sup> (white column), CD8<sup>+</sup> cells (black column) and CD19<sup>+</sup> (gray column), were determined by flow analysis (\*\* $P < 0.01$ , \*\*\* $P < 0.001$ ) (right panel).



cells are major histocompatibility complex (MHC) unrestricted cytotoxic cells<sup>38</sup> and they do not mediate relevant GVHD reactions.<sup>39</sup>

We first showed that the CD19xCD3 DART could effectively redirect human CIK cells from normal subjects and from patients against tumor B-cells *in vitro* (Fig. S4-A,-C). *In vivo*,

the engraftment of CD19<sup>+</sup>CD34<sup>+</sup> B-ALL cells leads to a rapid and massive infiltration of both lymphoid (spleen, bone marrow, etc.) and parenchymal organs (liver, kidneys, lungs etc.) and a blood stream invasion in all injected mice (Di Giacomo, personal communication). To evaluate the antitumor activity of the CD19xCD3 DART and CIK cells, NSG mice were

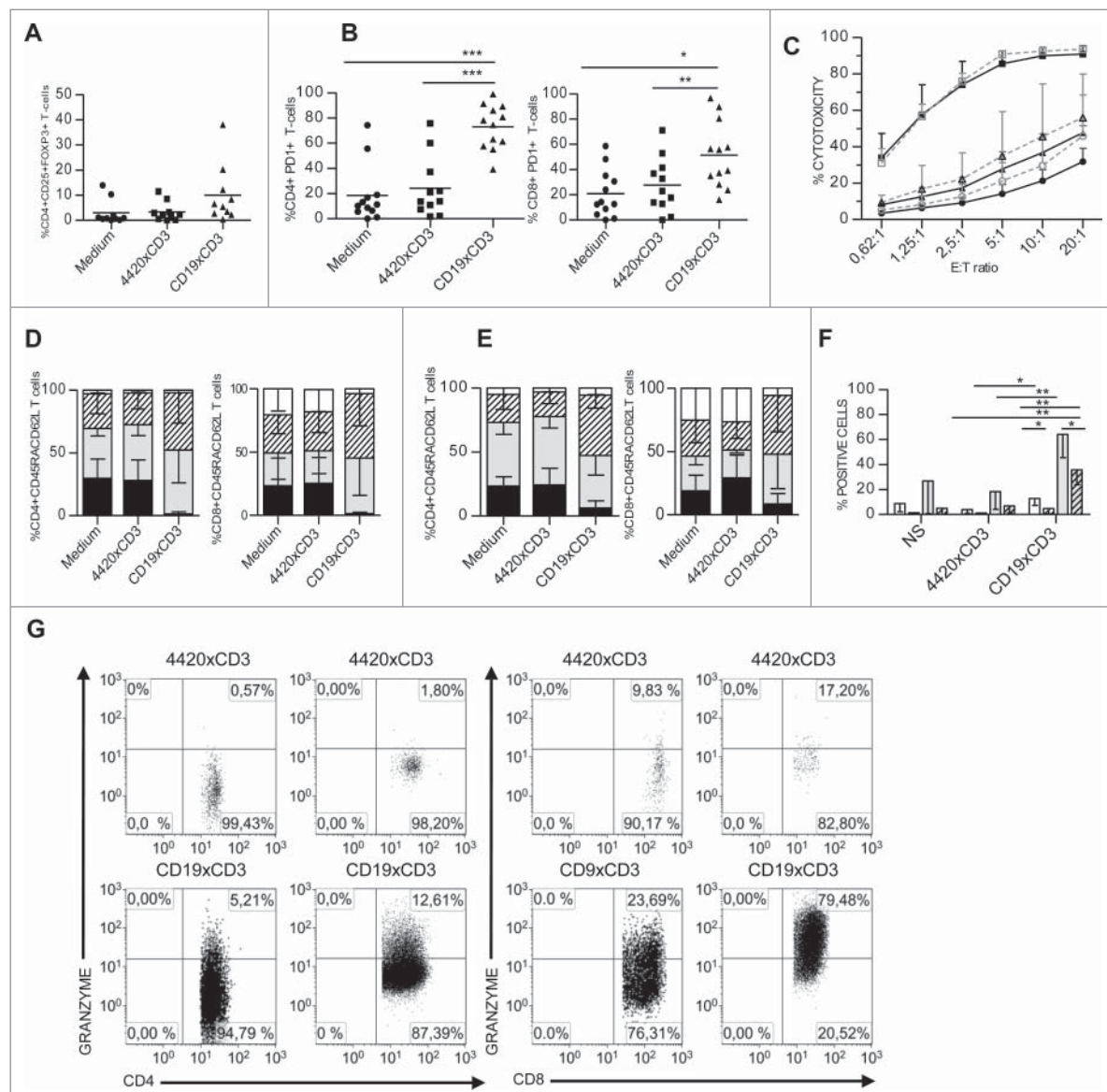


**Figure 3.** The effect of CD19xCD3 DART on proliferation and differentiation of autologous T-cells. (A) The percentage of regulatory T-cells was determined analyzing Foxp3 and CD25 expressions within the CD3<sup>+</sup>/CD4<sup>+</sup> cell subset (n = 10). (B) Expression of PD1 on CD4<sup>+</sup> (mean: 73.09 ± 17.73, right panel) and on CD8<sup>+</sup> (mean: 51.45 ± 26.27, left panel) T-cells (n = 12). Horizontal bars indicate the median value (\*P < 0.05, \*\*P < 0.01, \*\*\*P < 0.001). (C) Purified PD1<sup>-</sup> (solid black line) and PD1<sup>+</sup> (dotted gray line) cells (n = 3) from CD19xCD3 DART culture were co-cultured with CFSE-labeled MEC1 cells either alone (circles), in the presence of 4420xCD3 (triangles) or the CD19xCD3 (squares) DART (10 ng/ml). The cytotoxicity was determined at different ratio E:T by flow cytometric analysis after 16 hours of incubation (90.89 ± 4.6 for PD1<sup>-</sup> and 93.43 ± 0.4 for PD1<sup>+</sup> T-cells at 20:1 E:T and 33.94 ± 13.35 for PD1<sup>-</sup> and 31.06 ± 7.96 for PD1<sup>+</sup> T-cells at 0,62:1 E:T). Comparisons between CD4<sup>+</sup> or CD8<sup>+</sup> untreated or 4420xCD3 vs. CD19xCD3 DART treated were statistically significant (\*P < 0.05, \*\*P < 0.01, \*\*\*P < 0.001). (D-E) Subset distribution of naïve (CD45RA<sup>+</sup>CD62L<sup>+</sup> black), central memory (CD45RA<sup>-</sup>CD62L<sup>+</sup> gray), effector memory (CD45RA<sup>+</sup>CD62L<sup>-</sup> diagonal lines), terminal differentiated effector memory (CD45RA<sup>+</sup>CD62L<sup>-</sup> white) in CD4<sup>+</sup> (left panel) and CD8<sup>+</sup> T-cells (right panel) of fast responder (D, n = 8) and slow responder patients (E, n = 4). (F) Expression of granzyme B in CD4<sup>+</sup> of fast responder (n = 6, white column) and slow responder (n = 5, white column with diagonal lines) patients and in CD8<sup>+</sup> of fast responder (gray column) and slow responder (gray column with diagonal lines) patients (\*P < 0.05, \*\*P < 0.01). (G) Profile of granzyme B expression in CD4<sup>+</sup> (left panel) and CD8<sup>+</sup> T-cells (right panel) of the same patient (#22) during the course of disease. Dot plots show representative flow cytometric data in a slow responder phase (upper panel) and in a fast responder phase of the disease (lower panel). (H) Unsupervised analysis of enriched control and DART activated CD4<sup>+</sup> and CD8<sup>+</sup> cells demonstrated that both CD4<sup>+</sup> and CD8<sup>+</sup> cells after DART engagement cluster together. Spearman correlation was used as a distance metric for hierarchical clustering of the samples and genes. (I) DART induced activation leads to higher expression of cytotoxic genes (enrichment confirmed by GSEA analysis) in DART activated CD4<sup>+</sup> and CD8<sup>+</sup> cells vs control (p-value = 0.0002, FDR = 0.001). GSEA analysis (pre-ranked) was performed using log<sub>2</sub> fold-change of all genes between DART vs Control (Red: high, Green: low). (J) GSEA analysis between DART vs Control (log<sub>2</sub> fold change of all genes as the metric for GSEA pre-ranked) shows an enrichment for both memory T-cell associated and Th1 left panels) and NK associated genes (right panels). (K) Activated CD4<sup>+</sup> and CD8<sup>+</sup> DART cells display high levels of master regulators and (L) IFN-gamma transcripts.

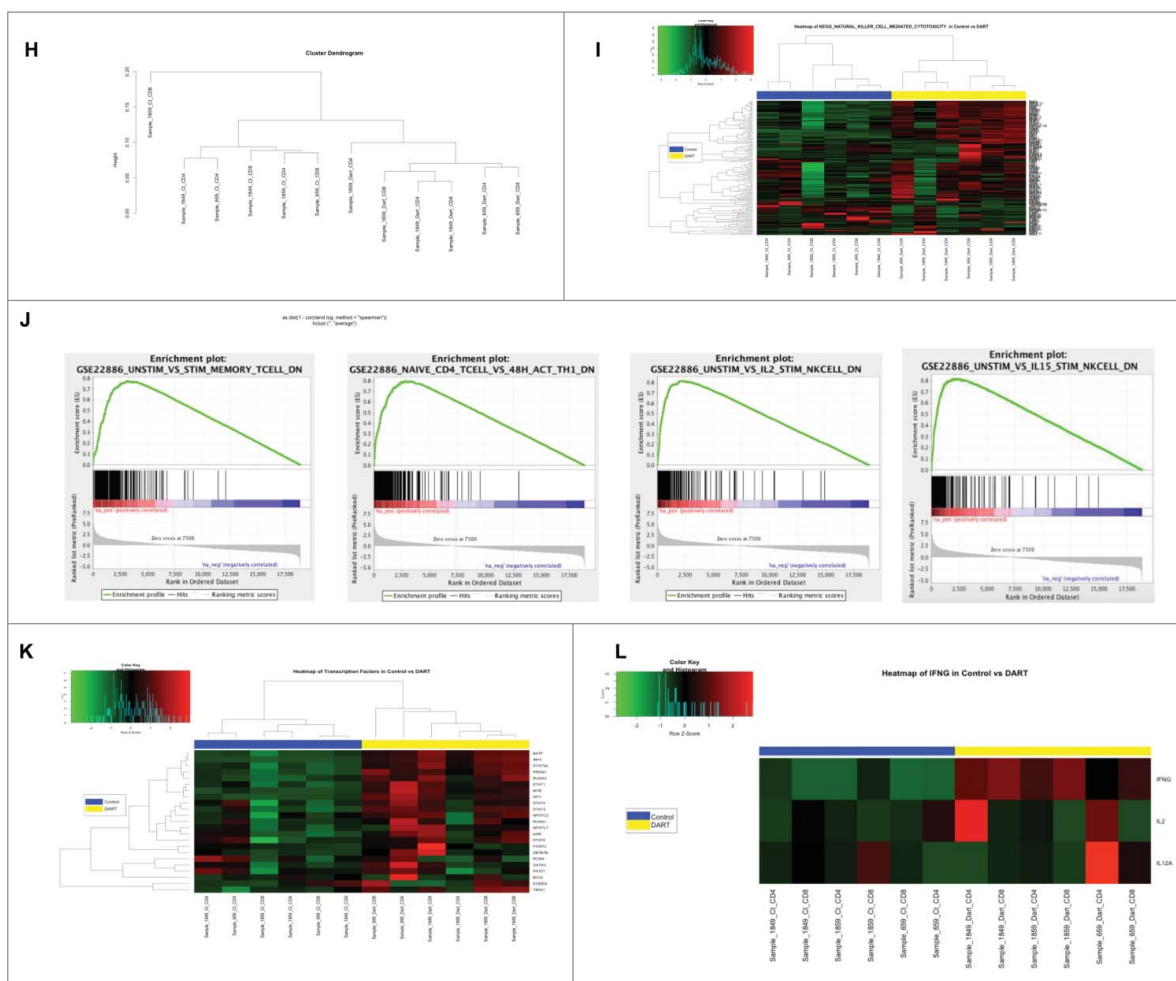
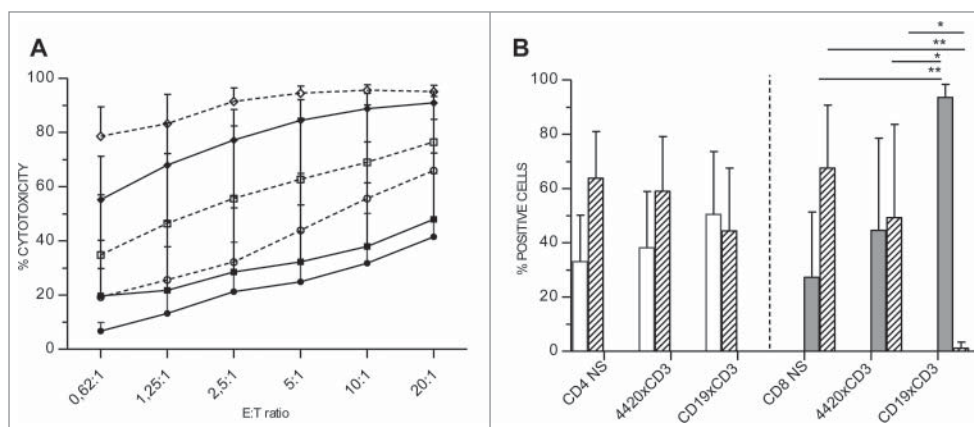


Figure 3. (Continued).

inoculated with a lethal dose of B-ALL ( $1 \times 10^6$ , i.v.) and then treated with serial doses of CIK cells ( $3 \times 10^6$ , i.p.). All mice injected with CIK had no sign of GVDH. CIK mice were randomized to receive either vehicle or CD19xCD3 DART

(Fig. 6A). By day 28, untreated mice showed a fatal leukemic phenotype. Meanwhile, mice treated with CIK cells displayed a partial response. Conversely, the combination of CIK and DART led to a robust anti-leukemia response ( $p = 0.0460$  vs.



**Figure 4.** CD19xCD3 DART induces differentiation of CD4<sup>+</sup> and CD8<sup>+</sup> cells into efficient cytotoxic effectors T-cells (A) Purified CD4<sup>+</sup> (solid black line) and CD8<sup>+</sup> (dotted black line) T-cells ( $n = 6$ ) from CD19xCD3 DART culture were co-cultured overnight with CFSE-labeled MEC1 cell line either alone (circles), in presence of 4420xCD3 (squares) or CD19xCD3 (diamonds) DART at 10 ng/ml. The cytotoxicity was determined at different ratio E:T by flow cytometric analysis after 16 hours of incubation. \* $P < 0.05$ , \*\* $P < 0.01$ , \*\*\* $P < 0.001$  at 2-tailed student t test. All comparisons between CD4<sup>+</sup> untreated vs. CD19xCD3 DART and CD8<sup>+</sup> untreated or 4420xCD3 vs. CD19xCD3 DART were statistically significant. (B) Purified CD4<sup>+</sup> and CD8<sup>+</sup> T-cells isolated from PBMC ( $n = 5$ ) were separately co-cultured with autologous purified CD19<sup>+</sup> either alone, with 4420xCD3 or CD19xCD3 DART at 10 ng/ml for 6 d. At day 6, the percentage of CD4<sup>+</sup> (white column), CD8<sup>+</sup> (gray column) and CD19<sup>+</sup> (white column with diagonal) was determined (day 0: 67,51  $\pm$  23,23 day 6: 1,09  $\pm$  2,2 with purified CD8<sup>+</sup> cells).

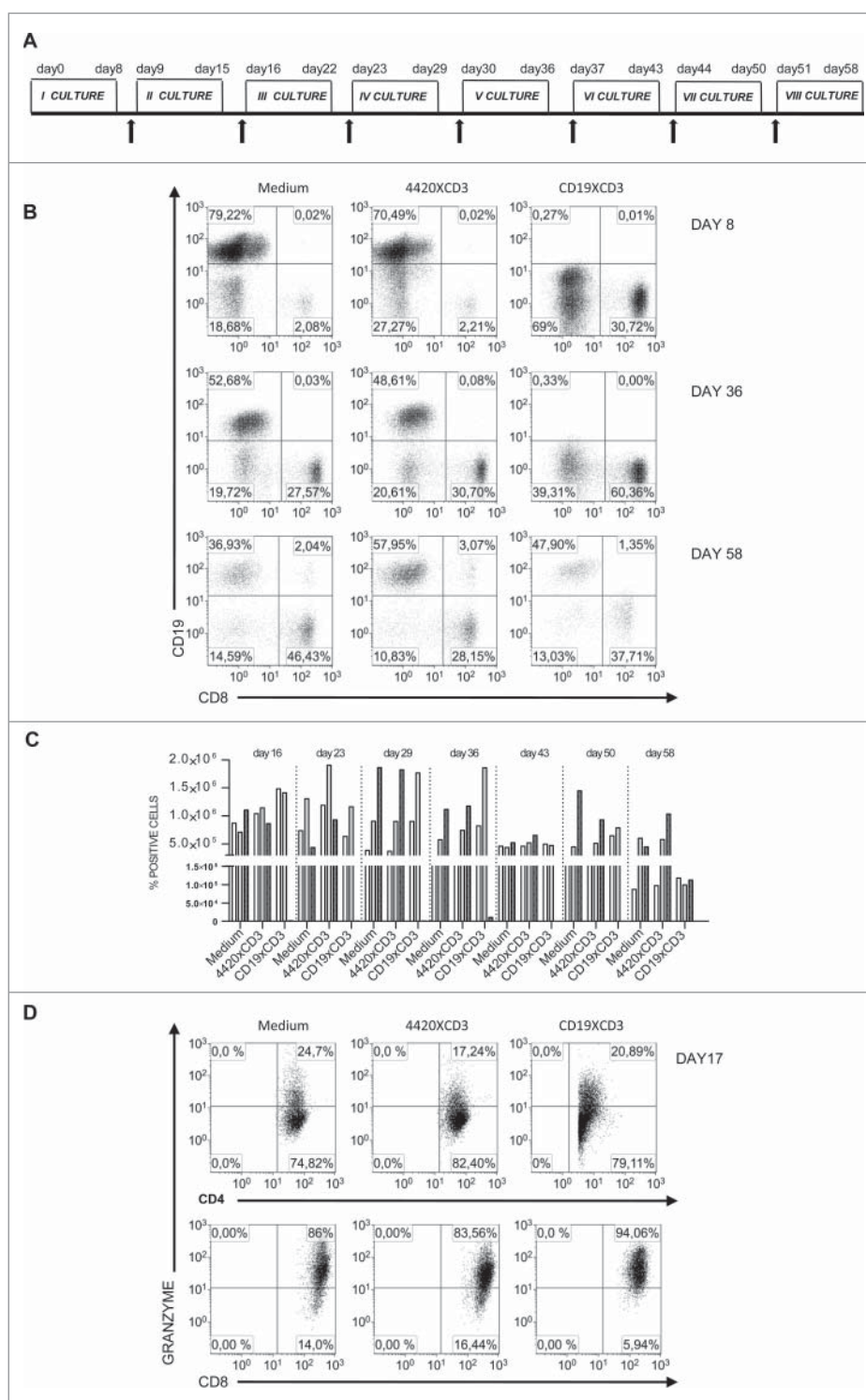


**Figure 5.** CD19xCD3 DART induces T-cell expansion and preserves cytotoxic capacity upon repeated challenges. (A) Schedule of repetitive culture of PBMC derived from a patient with CLL. PBMC were cultured with IL2 (20U/ml) and IL7 (5 ng/ml) and analyzed by flow cytometry. Fresh autologous CD19<sup>+</sup> cells (E:T ratio 1:5) were added as indicated (black arrows). (B) Representative flow cytometric dot plots of CD19<sup>+</sup> and CD8<sup>+</sup> cells after the first (day 8), fifth (day 36), and last (day 58) challenges with autologous B-CLL cells. (C) Absolute number of CD4<sup>+</sup> (white column), CD8<sup>+</sup> (gray column) and CD19<sup>+</sup> (black column) calculated at the end of every challenge. (D) Representative dot plots of intracellular Granzyme B expression as evaluated by flow cytometry at day 17 (III challenge). Values indicate the percentage of CD4<sup>+</sup>/granzyme-B<sup>+</sup> (upper panel) and the CD8<sup>+</sup>/granzymeB<sup>+</sup> population (lower panel).

CIK-treated mice Fig. 6B). All treated mice were alive at day 40 and were therefore killed to determine the extent of the response. The superior antitumor response of DART+CIK-treated mice was associated with a decreased fraction of CD19<sup>+</sup> blood circulating cells (Fig. 6C) and virtually undetectable

leukemic cells at autopsy (Fig. 6D). On the other hand, CIK-treated mice displayed infiltrating leukemic cells in the spleen, bone marrow, liver, kidneys and lungs. Both CIK-treated and, to a lesser extent, DART+CIK-treated mice showed some infiltrating cells within the bone marrow (Fig. 6E). By flow

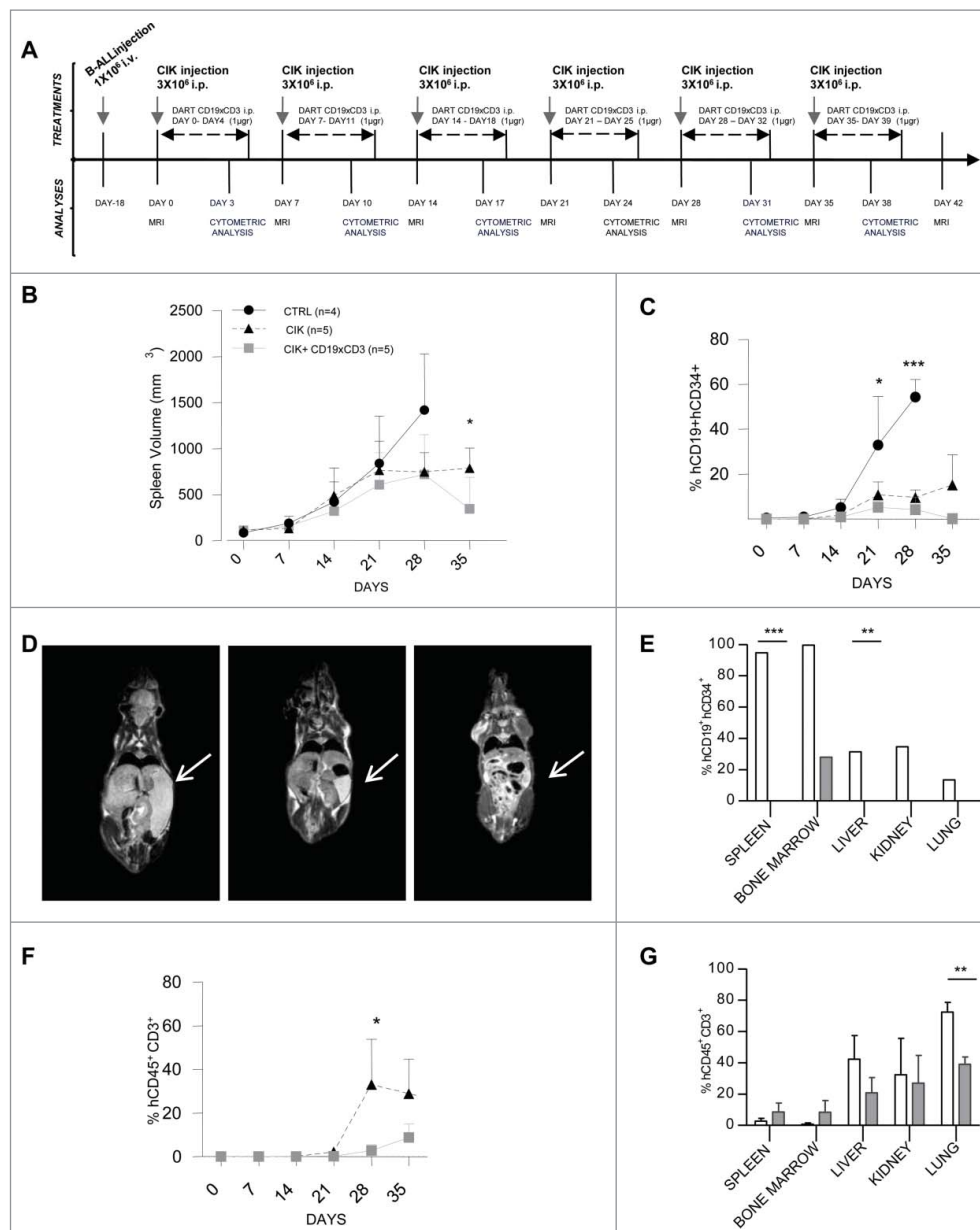


**Figure 6.** CD19xCD3 DART inhibit B-ALL patient derived tumor growth in NSG mice (A) Treatment schedule. NSG mice were inoculated with  $1 \times 10^6$  B-ALL cells (i.v) and treatment was initiated at day18 (mean spleen volume  $460 \text{ mm}^3$ ). CIK cells ( $3 \times 10^6$  cells/mouse) were infused i.p. once a week. CD19xCD3 DART ( $1 \mu\text{g}/\text{mouse}$ ) was injected (i.p.) daily. This protocol was repeated for 6 consecutive weeks. (B) Determination of spleen volume by MRI. Spleen volume of untreated mice (black line) or mice treated with CIK cells (dotted line) or with CIK cells + CD19xCD3 DART (gray line) was monitored once a week from day 0. Values correspond to mean  $\pm$  SD ( $^*p < 0.05$ ). (C) Mice were bled weekly and circulating human CD45<sup>+</sup>CD19<sup>+</sup>CD34<sup>+</sup> cells of untreated mice (black line), of mice treated with CIK cells (dotted line) or with CIK cells + CD19xCD3 DART (gray line) were analyzed by flow cytometry ( $^*P < 0.05$ ,  $^{***}P < 0.001$ ). (D) Representative MRI scans from untreated (left), CIK (middle) or CIK plus CD19xCD3 DART treated (right) mice. The scan of untreated mouse was performed at day 28 (day of euthanasia) and the scan of the treated mice (CIK cells or CIK cell plus CD19xCD3 DART) was performed at day 35. Spleens are highlighted and indicated by arrows. (E) At autopsy, the mean percentage of human CD45<sup>+</sup>CD19<sup>+</sup>CD34<sup>+</sup> cells of CIK (white column: spleen  $94,65 \pm 0,9$ ; bone marrow  $99,60 \pm 0,28$ ; liver  $31,30 \pm 5,23$ ; kidney  $34,54 \pm 47,32$  and lungs  $13,47 \pm 13,48$ ) or CIK + CD19xCD3 DART (gray column: bone marrow  $28,0 \pm 31,43$ ) treated mice was evaluated by FACS analysis. Values correspond to the mean  $\pm$  SD. ( $^{**}P < 0.01$ ;  $^{***}P < 0.001$ ). (F) Mice were bled weekly and circulating CD45<sup>+</sup>CD3<sup>+</sup> CIK cells of mice treated with CIK cells (dotted line) or with CIK cells and CD19xCD3 DART (gray line) were analyzed by flow cytometry. Statistical significance was determined by Student's t-test vs. the untreated control group ( $^*P < 0.05$ ). (G) The average percentage of CD45<sup>+</sup>CD3<sup>+</sup> CIK cells at the end point was evaluated by FACS analysis in the bone marrow, peripheral blood, spleen, liver, kidney and lung in mice treated with CIK (white column) or CIK and CD19xCD3 DART (gray column). Values correspond to the mean  $\pm$  SD ( $^{**}P < 0.01$ ).

cytometry, CIK cells were undetectable in the peripheral blood for up to 21 days, and then increased in CIK-treated as compared with CIK+DART mice (Fig. 6F), but at autopsy, CIK cells were readily detected in many organs (Fig. 6G).

We also studied a PDTX model from a chemo-refractory leukemic triple-hit DLBCL in which engrafted mice (s.c.  $1 \times 10^6$ ) die within 3 weeks post challenge (Fig. 7A). NSG mice were injected with a single bolus of CIK cells (i.p.  $5 \times 10^6$ )

before the inoculation of the lymphoma cells (s.c.). Mice were then treated bi-weekly with i.p. doses of CIK and CD19xCD3 DART (5 on/2 off for 7 wks, Fig. 7A) for 5 consecutive weeks and then CD19xCD3 DART only for 2 additional weeks. Tumor masses were readily detectable at day 10 in controls and progressively enlarged over time (Fig. 7B). Conversely, CIK+DART treatment suppressed tumor growth, leading to an improved overall survival ( $p = 0.0047$ , Fig. 7C). Two of 4

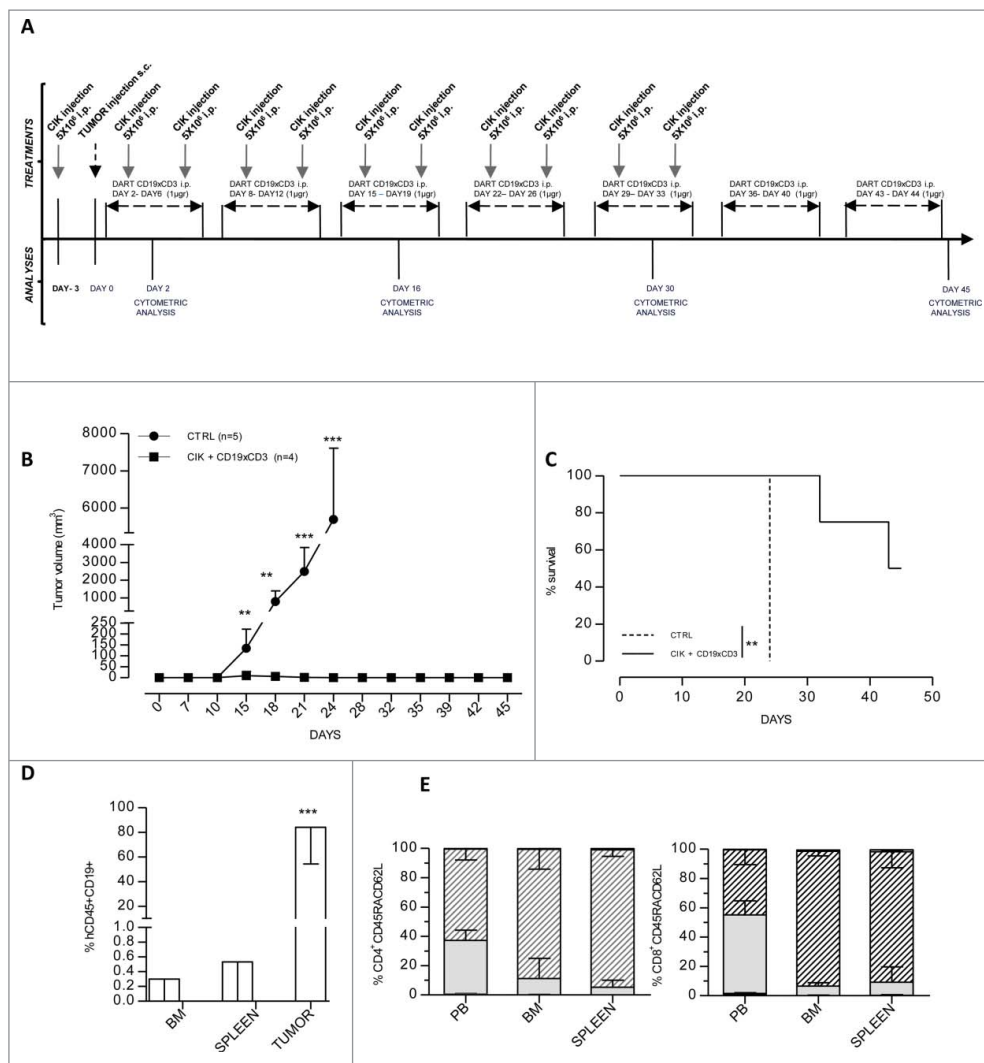


**Figure 7.** CD19xCD3 DART suppresses DLCL patient derived tumor growth in NSG mice (A) Treatment schedule. NSG mice were inoculated with  $5 \times 10^6$  CIK cells i.p. and after 3 d tissue samples of DLBCL PDTX were implanted (s.c.) on the ventral and/or dorsal regions. CIK cells ( $5 \times 10^6$  cells/mouse) were infused biweekly for 5 successive weeks. CD19xCD3 DART ( $1 \mu\text{g}/\text{mouse}$ ) was administered i.p., daily for 7 consecutive weeks. (B) Tumor volume progression was monitored once a week. Values correspond to the mean  $\pm$  SD. Statistical significance was determined by unpaired Student's t-test vs. the untreated control group (\*\*  $P < 0.01$ ; \*\*\*  $P < 0.001$ ). (C) Kaplan-Meier analysis of mice engrafted s.c. with DLBCL (black dotted line) and treated with CIK and CD19xCD3 DART (black line). Two CD19xCD3 DART animals without sign of disease were killed during treatment to histological analysis (black line). (D) The percentage of human CD45<sup>+</sup>CD19<sup>+</sup> at the end point was evaluated by FACS analysis in bone marrow, spleen, and tumor in untreated mice (white column) and in mice treated with CIK plus CD19xCD3 DART (gray column). Values correspond to mean  $\pm$  SD (\*\*\*)  $P < 0.001$ ). (E) Differentiation stage of CIK cells from mice group treated with CD19xCD3 DART at the end point. The left panel shows analysis performed on CD4<sup>+</sup> cells and right panel show analysis performed on CD8<sup>+</sup> cells.

mice of the CIK+DART group were killed for autopsy during treatment, whereas the other 2 mice were kept for follow up and were alive without sign of disease at day 45, when they also were killed for histological analysis. At autopsy, human CD45<sup>+</sup>CD19<sup>+</sup> lymphoma cells were detectable within the s.c. tumor masses ( $84.10 \pm 29.70$ ) or in distal compartments (spleen:  $0.53 \pm 0.66$ , bone marrow:  $0.29 \pm 0.344$ ) in untreated mice (Fig. 7D), while they were absent in CIK+DART animals. Effector memory CD3<sup>+</sup> cells were the predominant population in the bone marrow and spleen of these animals (Fig. 7E left panel),<sup>40</sup> whereas a distinct population of central memory cells was detectable only in the circulating pool (Fig. 7E right panel).

Collectively these pre-clinical studies demonstrated that CD19xCD3 DART and CIK cells represent a potentially effective tool for the treatment of primary human B-cell neoplastic disorders.

## Discussion

We have analyzed the therapeutic efficacy of a new CD19xCD3 DART antibody against a broad spectrum of primary human B-lymphoproliferative disorders *in vitro*. Our data demonstrate that the initial percentage of T-cells closely correlates with CD19xCD3 DART responsiveness. Nevertheless, effective responses could be achieved in all patients, regardless of the B-cell subtypes and the initial number of T lymphocytes. Both CD4<sup>+</sup> and CD8<sup>+</sup> effector cytotoxic cells were proven to be successfully generated and CIK cells armed with the bsAbs were effective in eradicating neoplastic B-cells both *in vitro* and *in vivo*.

Based on the rapidity by which neoplastic cells were eliminated, we stratified patients in "fast responders" and "slow responders." Although the T-cells of slow responders showed an initial "dysfunctional phenotype," longer/repetitive exposures

to DART resulted in the generation of powerful killer cells indicating that this phenotype was not due to an intrinsic dysfunction. This is relevant in the case of pluritreated patients,<sup>41</sup> who may have a limited T-cell repertoire, may be less prone to rapid polyclonal expansion and differentiation toward an effector phenotype,<sup>42</sup> and may be more susceptible to negative regulation by repressor elements.<sup>43</sup>

It is conceivable that the total number of T-cells as well as the intracytoplasmic granzyme expression levels represent *bona fide* biologic biomarkers predictor of response. Accordingly, the generation of cytolytic autologous CIK cells provide an alternative and powerful strategy for the debulking of B-cell neoplasms at early stages of treatment with bsAbs. These may lead to a rapid control of the disease,<sup>44,45</sup> while avoiding high degrees of T-cell activation that might result in significant toxicities.

Treatment with CD19xCD3 DART triggers the development of CD4<sup>+</sup> as well as CD8<sup>+</sup> effector T-cells, in all responders.<sup>46-50</sup> To date, cytotoxic CD4<sup>+</sup> T-cells have been identified in specific contexts characterized by a continuous antigen pressure, such as chronic infection<sup>51</sup> or autoimmune disorders.<sup>52</sup> The DART-mediated plasticity of mature CD4<sup>+</sup> implies that both CD4<sup>+</sup> and CD8<sup>+</sup> cooperate in target depletion, promoting strong and sustained anti-tumorigenic activity. Interestingly, DART-mediated differentiation of CD4<sup>+</sup> in killer cells required CD8<sup>+</sup>. This may due to the soluble factors and/or co-stimuli and/or direct cell-cell contact. Of note, once the cytolytic activity of CD4<sup>+</sup> cells was induced, it could be maintained over time independently of CD8<sup>+</sup> cells via repetitive CD19xCD3 DART exposures. This supports a model in which effectors are defined by their specific functional properties rather than their immunophenotypes.

The mechanisms driving cytotoxic CD4<sup>+</sup> effectors remain unclear and whether cytotoxic CD4<sup>+</sup> originate from different CD4<sup>+</sup> subpopulations or alternatively from a plastic rewiring remains largely untested.<sup>53,54</sup> Our transcriptomic analysis confirmed that the activation via CD19xCD3 DART upregulates Th1 and cytotoxic genes in CD4<sup>+</sup> cells, in line with the high levels of STAT4/T-Bet, which are known to sustain Th1 differentiation. Contrary to previous data, *Zbtb7b* transcripts were not reduced, demonstrating that bsAb-mediated plasticity does not change the fate of CD4<sup>+</sup> cells.<sup>53</sup>

DART exposure was associated with a reduction of naive T-cells and a shift toward a T<sub>CM</sub> and T<sub>EM</sub> phenotype. In adoptive cell-transfer with engineered T-cells, central memory T-cells rather than effector memory T-cells have a superior antitumor activity *in vivo*.<sup>55,56</sup> Thus, DART-expanded T-cells with both T<sub>CM</sub> and T<sub>EM</sub> phenotype may provide the optimal mix of effector subsets to mediate rapid and long lasting antitumor activity at the same time. In the clinical settings, antitumor activity could be influenced by CD4<sup>+</sup>CD25<sup>+</sup>T regulatory cells (T<sub>reg</sub>). In fact, in CD19-CAR T-cells models, transduced T<sub>reg</sub> can inhibit CAR-mediated cytotoxicity and cell proliferation.<sup>57</sup> Conversely, DART treatments should not lead to T-cell tolerance *in vivo*.

Since CD4<sup>+</sup> and CD8<sup>+</sup> T-cells can upregulate PD-1, a molecule that is linked to T-cell exhaustion and dysfunction,<sup>36</sup> the role of PD-1 following DART exposure needs to be explored.<sup>28</sup> Our data are in line with those of healthy individuals, in which PD-1 is upregulated by effector memory T-cells without an

exhausted gene signature.<sup>58</sup> The DART-mediated PD-1 upregulation most likely fits the model of an “activated” effector memory phenotype.<sup>59</sup>

Although bsAbs or engineered T-cells have recently emerged as powerful biologicals for the treatment of hematological and other human cancers,<sup>60</sup> resistant/escape mechanisms have been observed. These are due to alternative and/or multifactorial events. These include host related mechanisms such as poor T-cell expansions/function; conversely in a setting of strong immune responses/inflammatory phenotypes, tumor cells have been proven to use immune-suppressive strategies, which can block tumor-lyses/eradication (i.e. over-expression of PDL-1/PD1, CD47<sup>61</sup>). Interestingly, tumor cells may survive in immune privileged sanctuaries (i.e., testis, central nervous system), suggesting that compartmentalization can play a role in a minority of patients.<sup>19</sup> However, the most common escape scenario is linked to the loss of target epitopes as result of the loss of peptide recognition due to splice variants,<sup>62</sup> or alternatively to the ablation of tumor surface antigens.<sup>63</sup> Indeed, the loss of CD19 in B-cell neoplasms has been documented in both ALL as well in CLL patients, with the latter developing immunoblastic lymphoma.<sup>64</sup> In the case of CD19-relapses of ALL patients, individuals carrying chimeric fusions (MLL-1) have been found to relapse with acute myeloid leukemia. A phenomenon linked to either cell reprogramming, as demonstrated by the presence of identical Ig rearrangements of both original ALL and recurrent AML, or de-differentiation of putative uncommitted clones, bearing however the same translocation.<sup>65</sup> Thus, innovative approaches should be considered to counteract leukemia/lymphoma escape mechanisms. These include allogeneic stem cell transplantation following immune-therapies, which should improve tumor eradication via anti-leukemia effects, combined usage of bsAbs specifically recognizing different cancer antigens (i.e., CD123, CD22, CD20 etc.), and/or check point inhibitors.<sup>61</sup> These approaches are currently under investigation in multiple clinical trials.<sup>63</sup>

Preclinical studies performed in immunodeficient mice using bsAbs have tested PBMC effector cells and allogeneic cell lines as targets.<sup>28,29,66,67</sup> Although these models are informative, they display substantial hurdles to their widespread use. Here, we investigated the therapeutic potential of CD19xCD3 DART using PDTX models, that more faithfully recapitulate ALL and DLBCL, and using CIK cells, which display low and acceptable alloreactivity *in vivo*.<sup>39</sup> In absence of GVHD, we observed a strong antileukemic activity as a result of the high cytotoxic potential of redirected CIK cells and the effective trafficking of effector cells. Since an effective penetration of the effectors cells in the tumor environment is paramount,<sup>68</sup> as observed in our DLBCL PDTX model, understanding the mechanisms regulating effector trafficking will ultimately improve clinical performance and the design of conditioning regimens.

In conclusion, *in vitro* and *in vivo* data underscore the potent anti-tumoral activity of a CD19xCD3 DART for the treatment of CD19<sup>+</sup> B-cell disorders. We anticipate that monitoring the pre-therapy lymphoid host T-cells together with the expansion and recruitment of functional effectors can become informative biomarkers for the design of alternative therapies.

## Authorship

PC, AL, IL, RM, MD, SA, DB, and FdG, performed experiments. DG, MM, AC, and GI provided human samples. PC designed experiments and PC, ARE, RB, OE, EM, AC and GI analyzed experiments. PC, AC and GI wrote the manuscript. GRC, PAM, SJ and EB provided the CD19xCD3 DART and critical input in the analysis. ARG, RF, PWK edited the manuscript.

## Conflict-of-interest disclosure

G.R.C., P.A.M., S.J. and E.B. are employees of MacroGenics, Inc., the company developing CD3xCD3 DART, and receive salary and stock options as compensation for their employment. The other authors declare no competing financial interests.

## Acknowledgments

We are grateful to the Epigenomics Core members of Weill Cornell Medicine for their technical support and to Jason McCormick for his precious technical support and cell sorting (Mgr Flow Cytometry). G.I. is supported by the Italian Association for Cancer Research (5 × 1000 No. 10007); Regione Piemonte (ONCOPROT, CIPE 25/2005); and ImmOnc (BIO F.E. S.R. 2007/13), the Oncology Program of Compagnia di San Paolo, Torino, and Ricerca Finalizzata, Ministero della Salute. PC is a recipient of a fellowship from Gigi Ghirotti Foundation.

## ORCID

Giorgio Inghirami  <http://orcid.org/0000-0002-5298-6516>

## References

- Bassan R, Maino E, Cortelazzo S. Lymphoblastic lymphoma: an updated review on biology, diagnosis, and treatment. *Eur J Haematol* 2015; 96:447-60; PMID:26679753; <https://doi.org/10.1111/ejh.12722>
- Batlevi CL, Matsuki E, Brentjens RJ, Younes A. Novel immunotherapies in lymphoid malignancies. *Nat Rev Clin Oncol* 2016; 13:25-40; PMID:26525683; <https://doi.org/10.1038/nrclinonc.2015.187>
- Ansell SM. Hodgkin Lymphoma: Diagnosis and Treatment. *Mayo Clin Proc* 2015; 90:1574-83; PMID:26541251; <https://doi.org/10.1016/j.mayocp.2015.07.005>
- Ansell SM. Non-Hodgkin Lymphoma: Diagnosis and Treatment. *Mayo Clin Proc* 2015; 90:1152-63; PMID:26250731; <https://doi.org/10.1016/j.mayocp.2015.04.025>
- Zugmaier G, Klinger M, Schmidt M, Subklewe M. Clinical overview of anti-CD19 BiTE((R)) and ex vivo data from anti-CD33 BiTE((R)) as examples for retargeting T cells in hematologic malignancies. *Mol Immunol* 2015; 67:58-66; PMID:25883042; <https://doi.org/10.1016/j.molimm.2015.02.033>
- Wang Y, Zhang LL, Champlin RE, Wang ML. Targeting Bruton's tyrosine kinase with ibrutinib in B-cell malignancies. *Clin Pharmacol Ther* 2015; 97:455-68; PMID:25669675; <https://doi.org/10.1002/cpt.85>
- Salz T, Baxi SS, Raghunathan N, Onstad EE, Freedman AN, Moskowitz CS, Dalton SO, Goodman KA, Johansen C, Matasar MJ, et al. Are we ready to predict late effects? A systematic review of clinically useful prediction models. *Eur J Cancer* 2015; 51:758-66; PMID:25736818; <https://doi.org/10.1016/j.ejca.2015.02.002>
- Pui CH, Yang JJ, Hunger SP, Pieters R, Schrappe M, Biondi A, Vora A, Baruchel A, Silverman LB, Schmiegelow K, et al. Childhood Acute Lymphoblastic Leukemia: Progress Through Collaboration. *J Clin Oncol* 2015; 33:2938-48; PMID:26304874; <https://doi.org/10.1200/JCO.2014.59.1636>
- Stathis A, Younes A. The new therapeutical scenario of Hodgkin lymphoma. *Ann Oncol* 2015; 26:2026-33; PMID:26037796; <https://doi.org/10.1093/annonc/mdv256>
- Bivona TG, Doebele RC. A framework for understanding and targeting residual disease in oncogene-driven solid cancers. *Nat Med* 2016; 22:472-8; PMID:27149220; <https://doi.org/10.1038/nm.4091>
- Leavy O. Tumour immunology: A close-range dual hit for tumour immunity. *Nat Rev Immunol* 2012; 12:227; PMID:22362306; <https://doi.org/10.1038/nri3189>
- Pardoll DM. The blockade of immune checkpoints in cancer immunotherapy. *Nat Rev Cancer* 2012; 12:252-64; PMID:22437870; <https://doi.org/10.1038/nrc3239>
- Sharma P, Allison JP. The future of immune checkpoint therapy. *Science* 2015; 348:56-61; PMID:25838373; <https://doi.org/10.1126/science.aaa8172>
- Rosenberg SA, Restifo NP. Adoptive cell transfer as personalized immunotherapy for human cancer. *Science* 2015; 348:62-8; PMID:25838374; <https://doi.org/10.1126/science.aaa4967>
- Sharma P, Allison JP. Immune checkpoint targeting in cancer therapy: toward combination strategies with curative potential. *Cell* 2015; 161:205-14; PMID:25860605; <https://doi.org/10.1016/j.cell.2015.03.030>
- van der Stegen SJ, Hamieh M, Sadelain M. The pharmacology of second-generation chimeric antigen receptors. *Nat Rev Drug Discov* 2015; 14:499-509; PMID:26129802; <https://doi.org/10.1038/nrd4597>
- Armand P. Immune checkpoint blockade in hematologic malignancies. *Blood* 2015; 125:3393-400; PMID:25833961; <https://doi.org/10.1182/blood-2015-02-567453>
- Topp MS, Kufer P, Gokbuget N, Goebeler M, Klinger M, Neumann S, Horst HA, Raff T, Viardot A, Schmid M, et al. Targeted therapy with the T-cell-engaging antibody blinatumomab of chemotherapy-refractory minimal residual disease in B-lineage acute lymphoblastic leukemia patients results in high response rate and prolonged leukemia-free survival. *J Clin Oncol* 2011; 29:2493-8; PMID:21576633; <https://doi.org/10.1200/JCO.2010.32.7270>
- Topp MS, Gokbuget N, Zugmaier G, Degenhard E, Goebeler ME, Klinger M, Neumann SA, Horst HA, Raff T, Viardot A, et al. Long-term follow-up of hematologic relapse-free survival in a phase 2 study of blinatumomab in patients with MRD in B-lineage ALL. *Blood* 2012; 120:5185-7; PMID:23024237; <https://doi.org/10.1182/blood-2012-07-441030>
- Topp MS, Gokbuget N, Stein AS, Zugmaier G, O'Brien S, Bargou RC, Dombret H, Fielding AK, Heffner L, Larson RA, et al. Safety and activity of blinatumomab for adult patients with relapsed or refractory B-precursor acute lymphoblastic leukaemia: a multicentre, single-arm, phase 2 study. *Lancet Oncol* 2015; 16:57-66; PMID: 25524800; [https://doi.org/10.1016/S1470-2045\(14\)71170-2](https://doi.org/10.1016/S1470-2045(14)71170-2)
- Goebeler ME, Knop S, Viardot A, Kufer P, Topp MS, Einsele H, Noppeney R, Hess G, Kallert S, Mackensen A, et al. Bispecific T-Cell Engager (BiTE) Antibody Construct Blinatumomab for the Treatment of Patients With Relapsed/Refractory Non-Hodgkin Lymphoma: Final Results From a Phase I Study. *J Clin Oncol* 2016; 34:1104-11; PMID:26884582; <https://doi.org/10.1200/JCO.2014.59.1586>
- Ruella M, Gill S. How to train your T cell: genetically engineered chimeric antigen receptor T cells versus bispecific T-cell engagers to target CD19 in B acute lymphoblastic leukemia. *Expert Opin Biol Ther* 2015; 15:761-6; PMID:25640460; <https://doi.org/10.1517/14712598.2015.1009888>
- Braig F, Brandt A, Goebeler M, Tony HP, Kurze AK, Nollau P, Bumm T, Böttcher S, Bargou RC, Binder M. Resistance to anti-CD19/CD3 BiTE in acute lymphoblastic leukemia may be mediated by disrupted CD19 membrane trafficking. *Blood* 2016; 129:100-4; PMID:27784674; <https://doi.org/10.1182/blood-2016-05-718395>
- Kuo SR, Wong L, Liu JS. Engineering a CD123xCD3 bispecific scFv immunofusion for the treatment of leukemia and elimination of leukemia stem cells. *Protein Eng Des Sel* 2012; 25:561-9; PMID:22740616; <https://doi.org/10.1093/protein/gzs040>
- Schuster FR, Stanglmaier M, Woessmann W, Winkler B, Siepermann M, Meisel R, Schlegel PG, Hess J, Lindhofer H, Borkhardt A, et al. Immunotherapy with the trifunctional anti-CD20 × anti-CD3 antibody FBTA05 (Lymphomun) in paediatric high-risk patients with

- recurrent CD20-positive B cell malignancies. *Br J Haematol* 2015; 169:90-102; PMID:25495919; <https://doi.org/10.1111/bjh.13242>
26. Smits NC, Sentman CL. Bispecific T-Cell Engagers (BiTEs) as Treatment of B-Cell Lymphoma. *J Clin Oncol* 2016; 34:1131-3; PMID:26884583; <https://doi.org/10.1200/JCO.2015.64.9970>
  27. Johnson S, Burke S, Huang L, Gorlatov S, Li H, Wang W, Zhang W, Tuallon N, Rainey J, Barat B, et al. Effector cell recruitment with novel Fv-based dual-affinity re-targeting protein leads to potent tumor cytotoxicity and in vivo B-cell depletion. *J Mol Biol* 2010; 399:436-49; PMID:20382161; <https://doi.org/10.1016/j.jmb.2010.04.001>
  28. Chichili GR, Huang L, Li H, Burke S, He L, Tang Q, Jin L, Gorlatov S, Ciccarone V, Chen F, et al. A CD3xCD123 bispecific DART for redirecting host T cells to myelogenous leukemia: preclinical activity and safety in nonhuman primates. *Sci Transl Med* 2015; 7:289ra82; PMID:26019218; <https://doi.org/10.1126/scitranslmed.aaa5693>
  29. Moore PA, Zhang W, Rainey GJ, Burke S, Li H, Huang L, Gorlatov S, Veri MC, Aggarwal S, Yang Y, et al. Application of dual affinity retargeting molecules to achieve optimal redirected T-cell killing of B-cell lymphoma. *Blood* 2011; 117:4542-51; PMID:21300981; <https://doi.org/10.1182/blood-2010-09-306449>
  30. Kranz DM, Voss EW, Jr. Partial elucidation of an anti-hapten repertoire in BALB/c mice: comparative characterization of several monoclonal anti-fluorescyl antibodies. *Mol Immunol* 1981; 18:889-98; PMID:7335083; [https://doi.org/10.1016/0161-5890\(81\)90012-2](https://doi.org/10.1016/0161-5890(81)90012-2)
  31. Stacchini A, Aragno M, Vallario A, Alfarano A, Circosta P, Gottardi D, Faldella A, Rege-Cambrin G, Thunberg U, Nilsson K, et al. MEC1 and MEC2: two new cell lines derived from B-chronic lymphocytic leukaemia in prolymphocytoid transformation. *Leuk Res* 1999; 23:127-36; PMID: 10071128; [https://doi.org/10.1016/S0145-2126\(98\)00154-4](https://doi.org/10.1016/S0145-2126(98)00154-4)
  32. Crescenzo R, Abate F, Lasorsa E, Tabbo F, Gaudiano M, Chiesa N, Di Giacomo F, Spaccarotella E, Barbarossa L, Ercole E, et al. Convergent mutations and kinase fusions lead to oncogenic STAT3 activation in anaplastic large cell lymphoma. *Cancer Cell* 2015; 27:516-32; PMID:25873174; <https://doi.org/10.1016/j.ccell.2015.03.006>
  33. Subramanian A, Tamayo P, Mootha VK, Mukherjee S, Ebert BL, Gillette MA, Paulovich A, Pomeroy SL, Golub TR, Lander ES, et al. Gene set enrichment analysis: a knowledge-based approach for interpreting genome-wide expression profiles. *Proc Natl Acad Sci U S A* 2005; 102:15545-50; PMID:16199517; <https://doi.org/10.1073/pnas.0506580102>
  34. Teachey DT, Rheingold SR, Maude SL, Zugmaier G, Barrett DM, Seif AE, Nichols KE, Suppa EK, Kalos M, Berg RA, et al. Cytokine release syndrome after blinatumomab treatment related to abnormal macrophage activation and ameliorated with cytokine-directed therapy. *Blood* 2013; 121:5154-7; PMID:23678006; <https://doi.org/10.1182/blood-2013-02-485623>
  35. Klinger M, Brandl C, Zugmaier G, Hijazi Y, Bargou RC, Topp MS, Gökbuğut N, Neumann S, Goebeler M, Viardot A, et al. Immunopharmacologic response of patients with B-lineage acute lymphoblastic leukemia to continuous infusion of T cell-engaging CD19/CD3-bispecific BiTE antibody blinatumomab. *Blood* 2012; 119:6226-33; PMID:22592608; <https://doi.org/10.1182/blood-2012-01-400515>
  36. Wherry EJ, Kurachi M. Molecular and cellular insights into T cell exhaustion. *Nat Rev Immunol* 2015; 15:486-99; PMID: 26205583; <https://doi.org/10.1038/nri3862>
  37. King MA, Covassin L, Brehm MA, Racki W, Pearson T, Leif J, Laning J, Fodor W, Foreman O, Burzenski L, et al. Human peripheral blood leucocyte non-obese diabetic-severe combined immunodeficiency interleukin-2 receptor gamma chain gene mouse model of xenogeneic graft-versus-host-like disease and the role of host major histocompatibility complex. *Clin Exp Immunol* 2009; 157:104-18; PMID:19659776; <https://doi.org/10.1111/j.1365-2249.2009.03933.x>
  38. Schmidt-Wolf IG, Lefterova P, Mehta BA, Fernandez LP, Huhn D, Blume KG, Weissman IL, Negrin RS. Phenotypic characterization and identification of effector cells involved in tumor cell recognition of cytokine-induced killer cells. *Exp Hematol* 1993; 21:1673-9; PMID:7694868
  39. Baker J, Verneris MR, Ito M, Shizuru JA, Negrin RS. Expansion of cytolytic CD8(+) natural killer T cells with limited capacity for graft-versus-host disease induction due to interferon gamma production. *Blood* 2001; 97:2923-31; PMID:11342413; <https://doi.org/10.1182/blood.V97.10.2923>
  40. Elia AR, Circosta P, Sangiolo D, Bonini C, Gammaitoni L, Mastaglio S, Genovesi P, Geuna M, Avolio F, Inghirami G, et al. Cytokine-induced killer cells engineered with exogenous T-cell receptors directed against melanoma antigens: enhanced efficacy of effector cells endowed with a double mechanism of tumor recognition. *Hum Gene Ther* 2015; 26:220-31; PMID:25758764; <https://doi.org/10.1089/hum.2014.112>
  41. Scott DW, Gascoyne RD. The tumour microenvironment in B cell lymphomas. *Nat Rev Cancer* 2014; 14:517-34; PMID:25008267; <https://doi.org/10.1038/nrc3774>
  42. Christopoulos P, Follo M, Fisch P, Veelken H. The peripheral helper T-cell repertoire in untreated indolent B-cell lymphomas: evidence for antigen-driven lymphomagenesis. *Leukemia* 2008; 22:1952-4; PMID:18385751; <https://doi.org/10.1038/leu.2008.82>
  43. Fozza C, Corda G, Virdis P, Contini S, Barraqueddu F, Galleu A, Isoni A, Cossu A, Dore F, Careddu MG, et al. Derangement of the T-cell repertoire in patients with B-cell non-Hodgkin's lymphoma. *Eur J Haematol* 2015; 94:298-309; PMID:25040028; <https://doi.org/10.1111/ejh.12417>
  44. Sangiolo D, Mesiano G, Carnevale-Schianca F, Piacibello W, Aglietta M, Cignetti A. Cytokine induced killer cells as adoptive immunotherapy strategy to augment graft versus tumor after hematopoietic cell transplantation. *Expert Opin Biol Ther* 2009; 9:831-40; PMID:19463075; <https://doi.org/10.1517/14712590903005552>
  45. Introna M, Golay J, Rambaldi A. Cytokine Induced Killer (CIK) cells for the treatment of haematological neoplasms. *Immunol Lett* 2013; 155:27-30; PMID:24084446; <https://doi.org/10.1016/j.imlet.2013.09.017>
  46. Haas C, Krinner E, Brischwein K, Hoffmann P, Lutterbuse R, Schlereth B, Kufer P, Baeuerle PA. Mode of cytotoxic action of T cell-engaging BiTE antibody MT110. *Immunobiology* 2009; 214:441-53; PMID:19157637; <https://doi.org/10.1016/j.imbio.2008.11.014>
  47. Jensen M, Ernestus K, Kemshead J, Klehr M, Von Bergwelt-Baildon MS, Schinkoth T, Schultze JL, Berthold F. The bi-specific CD3 x NCAM antibody: a model to preactivate T cells prior to tumour cell lysis. *Clin Exp Immunol* 2003; 134:253-63; PMID:14616785; <https://doi.org/10.1046/j.1365-2249.2003.02300.x>
  48. Hoffman LM, Gore L. Blinatumomab, a Bi-Specific Anti-CD19/CD3 BiTE((R)) Antibody for the Treatment of Acute Lymphoblastic Leukemia: Perspectives and Current Pediatric Applications. *Front Oncol* 2014; 4:63; PMID:24744989; <https://doi.org/10.3389/fonc.2014.00063>
  49. Brischwein K, Schlereth B, Guller B, Steiger C, Wolf A, Lutterbuse R, Offner S, Locher M, Urbig T, Raum T, et al. MT110: a novel bispecific single-chain antibody construct with high efficacy in eradicating established tumors. *Mol Immunol* 2006; 43:1129-43; PMID:16139892; <https://doi.org/10.1016/j.molimm.2005.07.034>
  50. Wong R, Pepper C, Brennan P, Nagorsen D, Man S, Fegan C. Blinatumomab induces autologous T-cell killing of chronic lymphocytic leukemia cells. *Haematologica* 2013; 98:1930-8; PMID:23812940; <https://doi.org/10.3324/haematol.2012.082248>
  51. Brown DM. Cytolytic CD4 cells: Direct mediators in infectious disease and malignancy. *Cell Immunol* 2010; 262:89-95; PMID:20236628; <https://doi.org/10.1016/j.cellimm.2010.02.008>
  52. van de Berg PJ, van Leeuwen EM, ten Berge IJ, van Lier R. Cytotoxic human CD4(+) T cells. *Curr Opin Immunol* 2008; 20:339-43; PMID:18440213; <https://doi.org/10.1016/j.coi.2008.03.007>
  53. Mucida D, Huzain MM, Muroi S, van Wijk F, Shinnakasu R, Naoe Y, Reis BS, Huang Y, Lambalez F, Docherty M, et al. Transcriptional reprogramming of mature CD4(+) helper T cells generates distinct MHC class II-restricted cytotoxic T lymphocytes. *Nat Immunol* 2013; 14:281-9; PMID:23334788; <https://doi.org/10.1038/ni.2523>
  54. Reis BS, Rogoz A, Costa-Pinto FA, Taniuchi I, Mucida D. Mutual expression of the transcription factors Runx3 and ThPOK regulates intestinal CD4(+) T cell immunity. *Nat Immunol* 2013; 14:271-80; PMID:23334789; <https://doi.org/10.1038/ni.2518>
  55. Hinrichs CS, Borman ZA, Cassard L, Gattinoni L, Spolski R, Yu Z, Sanchez-Perez L, Muranski P, Kern SJ, Logun C, et al. Adoptively



- transferred effector cells derived from naive rather than central memory CD8<sup>+</sup> T cells mediate superior antitumor immunity. *Proc Natl Acad Sci U S A* 2009; 106:17469-74; PMID:19805141; <https://doi.org/10.1073/pnas.0907448106>
56. Klebanoff CA, Gattinoni L, Torabi-Parizi P, Kerstann K, Cardones AR, Finkelstein SE, Palmer DC, Antony PA, Hwang ST, Rosenberg SA, et al. Central memory self/tumor-reactive CD8<sup>+</sup> T cells confer superior antitumor immunity compared with effector memory T cells. *Proc Natl Acad Sci U S A* 2005; 102:9571-6; PMID:15980149; <https://doi.org/10.1073/pnas.0503726102>
57. Lee JC, Hayman E, Pegram HJ, Santos E, Heller G, Sadelain M, Brentjens R. In vivo inhibition of human CD19-targeted effector T cells by natural T regulatory cells in a xenotransplant murine model of B cell malignancy. *Cancer Res* 2011; 71:2871-81; PMID:21487038; <https://doi.org/10.1158/0008-5472.CAN-10-0552>
58. Duraiswamy J, Ibegbu CC, Masopust D, Miller JD, Araki K, Doho GH, Tata P, Gupta S, Zilliox MJ, Nakaya HI, et al. Phenotype, function, and gene expression profiles of programmed death-1(hi) CD8 T cells in healthy human adults. *J Immunol* 2011; 186:4200-12; PMID:21383243; <https://doi.org/10.4049/jimmunol.1001783>
59. Hong JJ, Amancha PK, Rogers K, Ansari AA, Villinger F. Re-evaluation of PD-1 expression by T cells as a marker for immune exhaustion during SIV infection. *PLoS One* 2013; 8:e60186; PMID:23555918; <https://doi.org/10.1371/journal.pone.0060186>
60. Zhang X, Yang Y, Fan D, Xiong D. The development of bispecific antibodies and their applications in tumor immune escape. *Exp Hematol Oncol* 2017; 6:12; PMID:28469973; <https://doi.org/10.1186/s40164-017-0072-7>
61. Cherkassky L, Morello A, Villena-Vargas J, Feng Y, Dimitrov DS, Jones DR, Sadelain M, Adusumilli PS. Human CAR T cells with cell-intrinsic PD-1 checkpoint blockade resist tumor-mediated inhibition. *J Clin Invest* 2016; 126:3130-44; PMID:27454297; <https://doi.org/10.1172/JCI83092>
62. Sotillo E, Barrett DM, Black KL, Bagashev A, Oldridge D, Wu G, Sussman R, Lanauze C, Ruella M, Gazzara MR, et al. Convergence of Acquired Mutations and Alternative Splicing of CD19 Enables Resistance to CART-19 Immunotherapy. *Cancer Discov* 2015; 5:1282-95; PMID:26516065; <https://doi.org/10.1158/2159-8290.CD-15-1020>
63. Ruella M, Maus MV. Catch me if you can: Leukemia Escape after CD19-Directed T Cell Immunotherapies. *Comput Struct Biotechnol J* 2016; 14:357-62; PMID:27761200; <https://doi.org/10.1016/j.csbj.2016.09.003>
64. Evans AG, Rothberg PG, Burack WR, Huntington SF, Porter DL, Friedberg JW, Liesveld JL. Evolution to plasmablastic lymphoma evades CD19-directed chimeric antigen receptor T cells. *Br J Haematol* 2015; <https://doi.org/10.1111/bjh.13562>
65. Gardner R, Wu D, Cherian S, Fang M, Hanafi LA, Finney O, Smithers H, Jensen MC, Riddell SR, Maloney DG, et al. Acquisition of a CD19-negative myeloid phenotype allows immune escape of MLL-rearranged B-ALL from CD19 CAR-T-cell therapy. *Blood* 2016; 127:2406-10; PMID:26907630; <https://doi.org/10.1182/blood-2015-08-665547>
66. Dreier T, Baeuerle PA, Fichtner I, Grun M, Schlereth B, Lorenczewski G, Kufer P, Lutterbüse R, Riethmüller G, Gjørstrup P, et al. T cell costimulus-independent and very efficacious inhibition of tumor growth in mice bearing subcutaneous or leukemic human B cell lymphoma xenografts by a CD19-/CD3- bispecific single-chain antibody construct. *J Immunol* 2003; 170:4397-402; PMID:12682277; <https://doi.org/10.4049/jimmunol.170.8.4397>
67. Aigner M, Feulner J, Schaffer S, Kischel R, Kufer P, Schneider K, Henn A, Rattel B, Friedrich M, Baeuerle PA, et al. T lymphocytes can be effectively recruited for ex vivo and in vivo lysis of AML blasts by a novel CD33/CD3-bispecific BiTE antibody construct. *Leukemia* 2013; 27:1107-15; PMID:23178753; <https://doi.org/10.1038/leu.2012.341>
68. Caruana I, Savoldo B, Hoyos V, Weber G, Liu H, Kim ES, Ittmann MM, Marchetti D, Dotti G. Heparanase promotes tumor infiltration and antitumor activity of CAR-redirected T lymphocytes. *Nat Med* 2015; 21:524-9; PMID:25849134; <https://doi.org/10.1038/nm.3833>